*Physics – Uspekhi* **40** (7) 701 – 716 (1997) 

*REVIEWS OF TOPICAL PROBLEMS* PACS numbers: 68.35.Ja, 68.35.Rh, **75.80.+q**, 77.80.Bh

# Magnetoacoustic surface waves in magnetic crystals near spin-reorientation phase transitions

Yu V Gulyaev, I E Dikshteĭn, V G Shavrov

## Contents



**Abstract. Theoretical and experimental work on magnetoacoustic surface waves in ferro- and antiferromagnets is reviewed. Results on the propagation of Rayleigh and Lamb magnetoelastic waves in a plate are presented within the framework of a rotation- and translation-invariant theory. Spectra of the shear surface magnetoacoustic waves (SSMAWs) caused by effects of magnetostriction and piezomagnetism are also considered with emphasis on the vicinity of reorientation phase transitions. The problem of the types of soft modes involved in phase transitions is discussed in detail. A comparison is made of experimental results and theoretical predictions on the propagation of Rayleigh waves in magnetic materials.**

## 1. Introduction

Magnetoelastic (ME) interaction plays an important role in the formation of many properties of magnetically ordered crystals (magnetic materials). In addition to the well-known and widely used magnetoacoustic resonance phenomena, ME interaction strongly affects magnetic resonance, quasistatic magnetization reversal, the nonlinear dynamics of magnetic materials, etc. [1]. The interaction between the magnetic (spin) and elastic subsystems of a magnetic material gives rise to coupled ME vibrations with very interesting physical properties [2 – 5].

Usually the ME interaction is weak and is determined by a dimensionless ME coupling parameter,

$$\zeta = \frac{\Delta c}{c}\,, \tag{1.1}$$

**Yu V Gulyaev, I E Dikshteĭn, V G Shavrov** Institute of Radio Engineering and Electronics, Russian Academy of Sciences,
ul. Mokhovaya 11, 103907 Moscow, Russia
Tel. (7-095) 203 24 26

Received 16 December 1996, revised 18 April 1997
*Uspekhi Fizicheskikh Nauk* **167** (7) 735 – 750 (1997)
Translated by E Yankovsky; edited by S N Gorin

where $c$ is the characteristic elastic constant, and $\Delta c$ is the variation of the constant caused by the ME interaction. For instance, for an easy-axis ferromagnet (in the absence of a magnetic field $H$),

$$\zeta = \frac{\omega_{\rm me}}{\omega_0} = \frac{H_{\rm me}}{H_{\rm A} + H_{\rm me}}\,. \tag{1.2}$$

Here $\omega_0$ is the gap in the spin wave spectrum, $\omega_{\rm me}$ is the ME contribution to this gap, $H_{\rm A}$ the magnetic anisotropy field, $H_{\rm me} = B^2/(cM_0)$ the magnetostriction field, $B$ the ME coupling constant, and $M_0$ the saturation magnetization. For typical magnetic materials ($M_0 \approx 10^2$ G, $c \approx 10^{12}$ erg cm$^{-3}$, $B \approx 10^7$ erg cm$^{-3}$, and $H_{\rm A} \approx 10^4$ Oe), the dimensionless ME coupling parameter is small: $\zeta \approx 10^{-4}$. However, there are physical situations in which the coupling of the magnetic and elastic subsystems is decisive. For instance, when the magnetic (spin) subsystem loses its stability, i.e., in the vicinity of magnetic orientational phase transitions (OPT), the energy of the ME interaction increases effectively in comparison to other types of energy, e.g., the magnetic anisotropy energy, which drops to zero as an OPT point is approached (accordingly, $H_{\rm A} \to 0$). In this case the ME coupling parameter $\zeta$ increases to unity. Hence, in the vicinity of an OPT, lattice vibrations and magnetic-moment oscillations should be considered in combination rather than separately, since their interrelationship is quite significant. This leads to effects that strongly influence the statistical, dynamic, thermodynamic, and other properties of magnetic crystals. In particular, an ME gap $\omega_{\rm me}$ appears in the spectrum of spin waves (quasimagnons) near an OPT [6 – 12], and for one of the quasiphonon modes the dispersion law and, hence, the speed of sound may change considerably [11 – 16]. Simple ideas may help to understand this situation. Suppose that we are dealing with two subsystems (e.g., magnetic and elastic), with each subsystem being in an activationless state (dashed lines in Fig. 1). When the interaction between the subsystems (magnetostriction) is

switched on, two types of motion develop. First, there are the oscillations of one subsystem with respect to the other (oscillations of the magnetic moment with respect to elastic strains). This is the activation branch of coupled vibrations (branch with an ME gap, represented by curve *1* in Fig. 1). Second, there are the activationless vibrations of the entire system as a whole. Clearly, these vibrations propagate at a speed lesser than that of the vibrations in each subsystem because, as a result of the interaction, each subsystem (with a linear dispersion law) is 'burdened' by the other (curve *2* in Fig. 1).

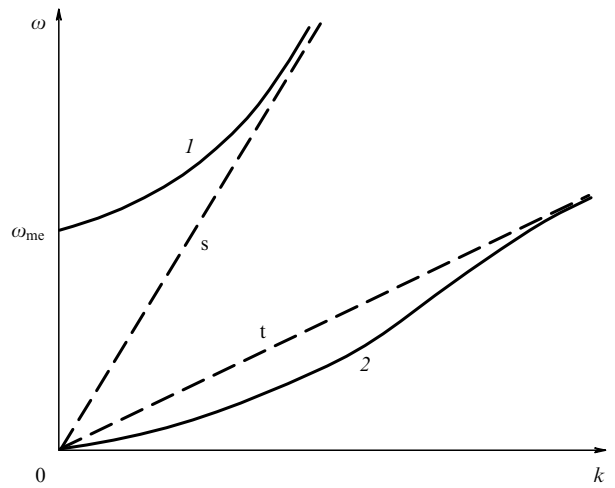


**Figure 1.** The spectrum of coupled ME waves in an antiferromagnet near an OPT (solid curves). The dispersion curves for the noninteracting spin (s) and elastic (t) waves are depicted by dashed curves ($\omega$ is the frequency, and $k$ is the wave number).

Experimentally, the decrease in the speed of sound in the vicinity of an OPT was observed in rhombohedral antiferromagnets, such as hematite and iron borate [17 – 21], rare-earth metals [22], and rare-earth orthoferrites [23 – 26]. The largest effect was observed in hematite [21] and terbium [23] (more than a 50% decrease in speed), and also in erbium orthoferrite in the low-temperature OPT region [26] (roughly a 25% decrease).

Apart from the speed of sound sharply decreasing near an OPT, there is also a sharp increase in sound attenuation [16, 27, 28]. However, attenuation manifests itself only in the immediate vicinity of an OPT and does not hinder the observation and utilization of the effect of decreasing speed of sound [28].

It was also discovered that in the vicinity of an OPT there is a giant increase in ME nonlinearity [29 – 31]: the magnetic contribution to the anharmonic elastic moduli increases by orders of magnitude. This leads to a number of nonlinear magnetoacoustic effects such as second-harmonic generation [32], parametric excitation of sound by sound and by a high-frequency magnetic field [33, 34], and magnetoacoustic convolution [35, 36].

Because of the strong distortion of the spectrum of coupled ME vibrations, the static and thermodynamic properties of magnetic materials undergo considerable changes near an OPT.

As an OPT point is approached, there occurs a sharp drop in static elastic constants, e.g., Young's modulus (an anomalous $\Delta E$ effect) [37] and an anomalous change in the distribution of magnetization and elastic stresses near defects of the crystal structure (impurities and dislocations) [38]. Features in the temperature behavior of the phonon entropy, internal energy, heat capacity, and other properties have also been observed. For instance, the $T^3$ law for phonon heat capacity becomes a $T^{5/2}$ law [39, 40].

Bulk (homogeneous) ME waves can propagate in infinite magnetic materials. In practice, however, we deal with finite crystals, in which surface (inhomogeneous) waves localized near free surfaces or interfaces between different media can arise in addition to bulk waves. The surface elastic waves known to propagate in nonmagnetic materials are the Rayleigh, Love, Stoneley, and Lamb waves [41 – 44]. In piezoelectric crystals, shear surface acoustic waves (SAWs) can arise, whose existence was predicted almost simultaneously by one of the present authors (Yu V G) [45] and by Bleustein [46].

Surface waves can also propagate in the purely magnetic subsystem of a magnetically ordered crystal. Damon and Eshbach [47, 48] were the first to study such waves in the magnetostatic approximation (without allowing for exchange interaction). These are slow waves (as are SAWs). The effect of exchange interaction on the spectrum of Damon – Eshbach waves was later taken into account by a number of researchers [49 – 54]. The conditions needed for the existence of surface spin waves in a purely exchange ferro- or antiferromagnetic material with a discontinuity in the exchange integral and partial magnetic-moment pinning at the surface were studied in Refs [55 – 58].

In magnetic crystals, we deal with modified magnetoelastic waves. Surface ME waves of the Rayleigh type propagating in a semi-infinite ferromagnet far from an OPT were studied in Refs [59 – 66]. Mathews and Van de Vaart [67, 69], Parekh [68], and Camley [70] studied Rayleigh and Love ME waves propagating in a thin ferromagnetic layer on a nonmagnetic substrate. Parekh and Bertoni [60, 62] studied Rayleigh ME waves propagating in insulating magnetic materials with a metallized surface, and Van de Vaart [69] and Parekh [71] studied the propagation of Love ME waves. Camley and Maradudin [72] discussed the behavior of Stoneley ME waves at the interface between two ferromagnets. Lamb ME waves propagating in a magnetic layer of finite thickness have been studied both experimentally and theoretically by many researchers [73 – 83]. Such waves are generated as a result of a resonant interaction of magnetostatic waves and acoustic Lamb waves in ferromagnetic plates and films. The interaction is most effective near the points of intersection of the dispersion curves of the corresponding noninteracting waves. The phase velocity of such hybrid waveguide-type waves propagating along the ferromagnetic surface is much higher than the speed of sound in an infinite medium. These 'fast ME waves' were first studied experimentally by Kazakov et al. [78].

The interaction of a Damon – Eshbach surface magnetostatic wave and a shear bulk elastic wave generates two coupled waves, a Damon – Eshbach ME wave (of quasimagnon type) and a shear surface magnetoacoustic wave (SSMAW) of quasiphonon type, with Parekh [84, 85] being the first to examine the latter type. Since the magnetostriction interaction has the same symmetry as the piezoelectric effect, these SSMAWs have the same structure as shear SAWs caused by the piezoelectric effect [45, 46]. The dispersion properties of the wave change upon the inversion of the dc magnetic field direction. The properties of surface ME waves

can be controlled externally (by a magnetic field or by elastic stresses).

SSMAWs due to the piezomagnetic effect in semi-infinite antiferromagnetic crystals were predicted and the properties studied by many researchers [86–92]. Since the symmetry of the piezomagnetic effect differs drastically from that of the piezoelectric or magnetostriction effect, SSMAWs differ dramatically from Gulyaev–Bleustein waves (GBW). In uniaxial antiferromagnets, an SSMAW in this case is two-component, i.e., it has a short-range component and a long-range component (long compared to the wavelength) of elastic displacement (the only component of a GBW is long-range). Thus, such a wave combines the merits of a Rayleigh wave at low frequencies and those of a GBW at high frequencies.

Ioffe [93] predicted the existence of a new type of ME wave propagating in a thin plate of a piezomagnetic antiferromagnet. They found that in the nonlinear limit such a wave forms a soliton.

Surface ME waves may lose energy by radiation from the surface into the bulk [83]. For instance, Parekh's SSMAW [84] emits exchange waves, with the pinning of the spin at the surface increasing the attenuation of such waves. Attenuation of a Damon–Eshbach wave is due to sound emission [83].

Most researchers studying magnetoacoustic phenomena ignore the effects of violation of the rotational invariance of the crystal's energy in a magnetic field. It is usually assumed that the free energy depends only on the symmetric part of the distortion tensor, $u_{i,k} = \partial u_i/\partial x_k$, i.e., on the strain tensor

$$e_{ik} = \frac{1}{2}\left(\frac{\partial u_i}{\partial x_k} + \frac{\partial u_k}{\partial x_i}\right),$$

where $\mathbf{u}$ is the displacement vector. However, within this approach the free energy is invariant with respect to translation of the volume elements of the crystal, but it is not invariant with respect to a local rotation of such elements. When sound propagates in a magnetic material, the volume elements of the medium turn locally together with the magnetic anisotropy axes, which naturally increases the energy of the crystal. Examining this problem in a rigorous setting requires building a consistent translation- and rotation-invariant theory that should also allow for the dependence of energy on the antisymmetric part of the distortion tensor

$$\omega_{ik} = \frac{1}{2}\left(\frac{\partial u_i}{\partial x_k} - \frac{\partial u_k}{\partial x_i}\right)$$

related to the rotation of small volume elements with respect to each other upon an inhomogeneous deformation of the crystal [94–98].

Effects associated with allowance for the $\omega_{ik}$ tensor manifest themselves both in massive and in limited specimens. In massive specimens the rotation-invariant theory predicts only a small difference between the speeds of transverse sound propagating along the easy axis of a uniaxial crystal or at right angles to this axis [99–101]. Melcher [99] was the first to observe this effect in a massive tetragonal antiferromagnet $MnF_2$, with the antiferromagnetism vector $\mathbf{L}$ directed along the $z$ axis. He found the experimental dependence of the relative variation of the elastic constant, $\Delta c_{44}/c_{44}$, on the magnetic field strength $H$ (i.e., on the parameter $H^2/(H_{sf}^2 - H^2)$, where $H_{sf}$ is the spin-flop transition field) for transverse waves with $\mathbf{k} \parallel \mathbf{L}$ and with $\mathbf{k} \perp \mathbf{L}$ (Fig. 2). Figure 2 shows that as the field strength

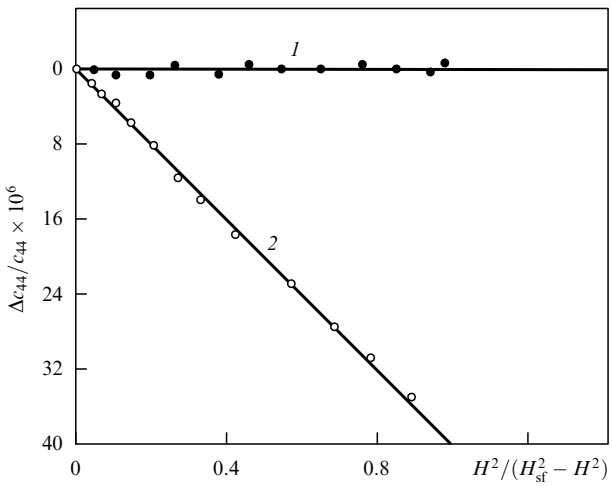


**Figure 2.** Dependence of the relative change in the transverse elastic constant $\Delta c_{44}/c_{44}$ on the parameter $H^2/(H_{sf}^2 - H^2)$ in $MnF_2$ at $T = 4.2$ K and frequency $\omega = 30$ MHz: *1* is the transverse mode with $\mathbf{k} \parallel [100] \parallel \mathbf{L}$ and $\mathbf{u} \parallel [001]$, and *2* is the transverse mode with $\mathbf{k} \parallel [001] \perp \mathbf{L}$ and $\mathbf{u} \parallel [100]$ [99, 100].

increases, the difference in the speeds of the two waves increases too, and reaches its maximum value near the spin-flop transition. For magnetic plates of finite thickness, Bar'yakhtar et al. [102, 103] predicted a new effect consisting in a change in the dispersion law of the flexural wave: the law in the long-wave range is transformed into a linear (sonic) law.

For all the surface waves we have discussed so far, ME coupling is important only near magnetoacoustic resonance. The ME coupling effect becomes stronger and in some cases leads to new results when the magnetic subsystem approaches an OPT. The propagation of ME waves near an OPT have been studied quite extensively.

For instance, Gerus and Tarasenko [104] found that as an OPT is approached, the speed of propagation of a Rayleigh wave decreases in proportion to $\xi^{1/2}$ (where $\xi = 1 - \zeta$ is a parameter characterizing the closeness to the OPT point), while the attenuation factor $\gamma = \mathrm{Im}\, k$ and the penetration depth $\Lambda$ increase: $\gamma \propto \xi^{-3/2}$ and $\Lambda \propto \xi^{-1/2}$. Since in the process the elliptic polarization of the wave changes to transverse, at the OPT point the Rayleigh wave becomes a transverse bulk wave.

The propagation of Rayleigh waves near the OPT has been studied in a number of experiments [105–108]. Easy-plane antiferromagnets, such as hematite and iron borate, exhibited a strong dependence of the speed of propagation of such a wave on the magnitude and direction of the magnetic field in the basal plane. The maximum decrease in the speed of propagation of a Rayleigh wave observed in the experiment by Kukhtin et al. [105] amounted to 35%.

Research into the propagation of Rayleigh ME waves in hematite revealed nonlinear effects such as generation of the second acoustic harmonic [109] and acoustic convolution of these waves [110, 111]. As an OPT point is approached, the efficiency of power conversion from the fundamental wave to the second harmonic and the convolution amplitude grow. The specific features of the Rayleigh second harmonic propagation discovered by Krasil'nikov et al. [109] were explained theoretically by Buchel'nikov et al. [112].

A rigorous rotation- and translation-invariant theory was used in Ref. [113] to study the propagation of Lamb and

Rayleigh waves in the vicinity of an OPT point in a magnetic plate placed in a magnetic field. Here, allowance for the rotational invariance of the energy of the magnetic crystal with respect to the crystal's orientation in space changes the spectrum of the coupled ME waves. Whereas in the zero magnetic field the soft modes of the magnetic plate near an OPT are one of the transverse bulk modes and a Rayleigh wave, in a nonzero magnetic field the flexural ME mode is the soft mode.

The SSMAWs related to magnetostriction in uniaxial magnetic materials near an OPT have been studied by a number of researchers [91, 92]. They found that as an OPT point is approached, the speed of SSMAW propagation drops to a certain critical value, and the depth of its penetration into the crystal diminishes too.

At present we can consider the propagation of linear and nonlinear ME waves in massive specimens in the vicinity of an OPT thoroughly studied and covered in many reviews [11, 12, 30, 31, 98], but this is certainly not the case with surface and bulk ME waves in limited crystals, although such studies are important from the theoretical viewpoint and for practical reasons. Considerable variation in the speed of sound and the important role that nonlinear processes play near an OPT make such crystals a promising material for use in electronic devices. The effectiveness of such devices can be raised considerably by using surface ME waves, since the energy of such waves is concentrated within a thin surface layer. From the scientific viewpoint, the study of the spectra of ME waves in limited specimens of magnetic materials makes it possible to determine the type of soft mode used in the OPT. In particular, in thin plates it is the flexural ME mode that proves to be the soft mode.

This review covers the theoretical aspects of studies of Rayleigh and Lamb ME waves propagating in ferro- and antiferromagnetic plates and of SSMAWs due to magnetostriction and piezomagnetism. The focus is on the OPT region. We also discuss the results of related experimental work.

## 2. The energy and the equations of motion of a magnetoelastic medium with free surfaces

### 2.1 Ferromagnet

The usual approach to studying the spectrum of low-frequency vibrations of interacting magnetic and elastic subsystems is to introduce the nonequilibrium thermodynamic potential [98]

$$\mathcal{F} = \int F(\mathbf{r})\,\mathrm{d}^3 r \tag{2.1}$$

whose density consists of magnetic, elastic and magnetoelastic components:

$$F(\mathbf{r}) = F_{\mathrm{m}}(\mathbf{r}) + F_{\mathrm{e}}(\mathbf{r}) + F_{\mathrm{me}}(\mathbf{r})\,. \tag{2.2}$$

Here

$$F_{\mathrm{m}} = \frac{1}{2}\,A_{ik}\,\frac{\partial \mathbf{m}}{\partial x_i}\cdot\frac{\partial \mathbf{m}}{\partial x_k} + K_{ik}^{(1)} m_i^* m_k^* + K_{iklm}^{(2)} m_i^* m_k^* m_l^* m_m^* + \ldots - \mathbf{M}\cdot\mathbf{H} - \frac{1}{2}\,\mathbf{M}\cdot\mathbf{H}_{\mathrm{D}}\,, \tag{2.3}$$

$$F_{\mathrm{e}} = \frac{1}{2}\,c_{iklm}\mathcal{E}_{ik}\mathcal{E}_{lm}\,, \tag{2.4}$$

$$F_{\mathrm{me}} = B_{iklm} m_i\, m_k \mathcal{E}_{lm} + G_{iklm}\,\frac{\partial \mathbf{m}}{\partial x_i}\cdot\frac{\partial \mathbf{m}}{\partial x_k}\,\mathcal{E}_{lm} + \ldots\,, \tag{2.5}$$

where $A$ is the nonuniform exchange constant, $K$ and $B$ are the anisotropy and magnetostriction constants in a locally rotated (due to deformation) system of coordinates, $c$ are the elastic constants, $G$ are the exchange-magnetostriction constants, $\mathbf{m}$ and $\mathbf{m}^* = \hat{R}^{-1}\mathbf{m}$ are unit vectors of magnetization $\mathbf{M}$ in the laboratory and local coordinate systems (the latter rotates together with its volume element upon an inhomogeneous deformation of the crystal),

$$\hat{R} = \hat{I} + \hat{\omega} + \frac{1}{2}(\hat{\omega}^2 + \hat{e}\hat{\omega} + \hat{\omega}\hat{e}) + O(u_{i,k}^3) \tag{2.6}$$

is the local rotation tensor, $\mathcal{E}$ is the total strain tensor [99], $I$ is the unit tensor, and $\mathbf{H}_{\mathrm{D}}$ is the demagnetizing field. The detailed form of the energy density (2.2) is determined by the symmetry of the crystal.

The equilibrium values $\mathbf{M}^{(0)}$ and $\mathcal{E}^{(0)}$ can be found by minimizing the thermodynamic potential. To find the spectrum of ME vibrations we must shift to the laboratory coordinate system and use the Landau – Lifshitz equation with a Hilbert dissipative term

$$\frac{\partial \mathbf{M}}{\partial t} + \frac{\partial(\mathbf{M}\dot{u}_k)}{\partial x_k} = g\left[\mathbf{M}\times\mathbf{H}_{\mathrm{eff}}\right] - \frac{r}{M_0}\left[\mathbf{M}\times\dot{\mathbf{M}}\right], \tag{2.7}$$

the equations of the continuum dynamics

$$\rho\ddot{u}_i = \frac{\partial(\sigma_{ik} + \sigma'_{ik})}{\partial x_k} + \frac{\mathbf{M}\cdot\partial\mathbf{H}_{\mathrm{eff}}}{\partial x_i}\,, \tag{2.8}$$

and the equations of magnetostatics

$$\nabla\times\mathbf{H}_{\mathrm{D}} = 0\,, \qquad \operatorname{div}\mathbf{H}_{\mathrm{D}} = -4\pi\operatorname{div}\mathbf{M}\,, \tag{2.9}$$

where $g > 0$ is the gyromagnetic ratio, $\mathbf{H}_{\mathrm{eff}} = -\delta\mathcal{F}/\delta\mathbf{M}$ is the effective field, $r$ is the dimensionless attenuation factor of the magnetic subsystem, $\sigma_{i,k} = \partial F/\partial u_{i,k}$ is the elastic stress tensor, $\sigma'_{i,k} = \eta_{iklm}u_{l,m}$ is the dissipative stress tensor, $\eta$ is the viscosity tensor, and $\rho$ is the density of the ferromagnetic material.

The above system of equations must be solved subject to the conditions that (1) there are no mechanical stresses and a normal component of the energy flux density; and (2) the normal component of the magnetic induction and the tangential component of the magnetic field are continuous at the ferromagnet – vacuum boundary:

$$\left\{\sigma_{i,k}n_k + (\mathbf{M}\cdot\mathbf{H}_{\mathrm{eff}})n_i\right\}\Big|_{\mathrm{s}} = 0\,, \tag{2.10}$$

$$\frac{\partial F}{\partial(\partial M_i/\partial x_k)}\,n_k\Big|_{\mathrm{s}} = 0\,, \tag{2.11}$$

$$B_{\mathrm{n}}^{\mathrm{int}}\Big|_{\mathrm{s}} = B_{\mathrm{n}}^{\mathrm{ext}}\Big|_{\mathrm{s}}\,, \tag{2.12}$$

$$H_{\tau}^{\mathrm{int}}\Big|_{\mathrm{s}} = H_{\tau}^{\mathrm{ext}}\Big|_{\mathrm{s}}\,. \tag{2.13}$$

The spin and elastic vibrations are related through magnetostrictive and ponderomotive forces [97]. The second term on the left-hand side of Eqn (2.7), the third term on the right-hand side of Eqn (2.8), and the second term on the left-hand side of boundary condition (2.10) are responsible for the ponderomotive forces. In this review we examine magnetic crystals in which magnetostriction is high ($B/M_0^2 \gg 1$), so that the effect of ponderomotive forces on the magnetoelastic properties can be ignored.

### 2.2 Antiferromagnet

This review deals with the problem of magnetoacoustics of two-sublattice collinear (or weakly noncollinear) antiferromagnets, in which far from the magnetic ordering point (the Néel point $T_N$) the magnetic moments of the sublattices, $\mathbf{M}_1$ and $\mathbf{M}_2$, meet the condition $|\mathbf{M}_1| = |\mathbf{M}_2| = M_0$. Magnetoanisotropy fields of the relativistic and exchange-relativistic origin and the commonly used external magnetic fields are low compared to the exchange fields $H_E \simeq 10^6 - 10^7$ Oe. Therefore, we can assume that

$$|\mathbf{m}| \ll |\mathbf{l}|\,, \qquad l^2 \approx 1\,, \tag{2.14}$$

where

$$\mathbf{m} = \frac{\mathbf{M}_1 + \mathbf{M}_2}{2M_0} \quad \text{and} \quad \mathbf{l} = \frac{\mathbf{M}_1 - \mathbf{M}_2}{2M_0}$$

are the ferro- and antiferromagnetic vectors, respectively.

The nonequilibrium thermodynamic potential of an antiferromagnet is given by Eqns (2.1) and (2.2). We can then write the magnetic contribution as

$$F_m = \frac{1}{2} E\mathbf{m}^2 + \frac{1}{2} A_{ik} \frac{\partial \mathbf{l}}{\partial x_i} \cdot \frac{\partial \mathbf{l}}{\partial x_k} + K_{ik}^{(1)} l_i^* l_k^* + K_{iklm}^{(2)} l_i^* l_k^* l_l^* l_m^* + D_{ik} m_i^* l_k^* - 2M_0 \mathbf{m} \cdot \mathbf{H} - M_0 \mathbf{m} \cdot \mathbf{H}_D\,, \tag{2.15}$$

where $E$ and $D$ are the uniform exchange and Dzyaloshinskiĭ constants, respectively, and the definition of $\mathbf{l}^*$ is similar to that of $\mathbf{m}^*$, i.e., $\mathbf{l}^* = R^{-1}\mathbf{l}$.

The elastic contribution is given by Eqn (2.4).

As is known, in antiferromagnets, in addition to the magnetostriction mechanism, there is another — piezomagnetic — mechanism of ME coupling [114–116]. Since the magnetostriction and piezomagnetism tensors are invariant with respect to different crystal symmetry elements, we arrive at different physical results for the corresponding surface magnetoacoustic waves. The ME contribution to the thermodynamic potential density of an antiferromagnet can be written as

$$F_{me} = A_{iklm} m_i^* m_k^* \mathcal{E}_{lm} + B_{iklm} l_i^* l_k^* \mathcal{E}_{lm} + C_{iklm} m_i^* l_k^* \mathcal{E}_{lm}\,. \tag{2.16}$$

Generally speaking, this formula is valid for any two-sublattice magnetic material, including crystals with nonequivalent magnetic sublattices, i.e., ferrimagnets. When an antiferromagnet is involved, the first two terms on the right-hand side of Eqn (2.16), which pertain to magnetostriction, are invariant under permutations of the magnetic moments of the sublattices, while the third, piezomagnetic term changes its sign under such an operation.

In the case at hand, Eqn (2.8) retains its form (here, we also ignore ponderomotive forces), Eqn (2.7) is replaced by similar equations for each sublattice, and in (2.9) $\mathbf{M}$ must be replaced by $2M_0\mathbf{m}$.

## 3. Rayleigh and Lamb magnetoelastic waves in a magnetic plate

We begin our study of surface ME waves by an analysis of the propagation of Rayleigh and Lamb waves in a magnetic plate. We illustrate the main laws governing the propagation of such waves with the example of orthorhombic ferro- and antiferromagnets. The results can easily be generalized to the case of tetragonal and cubic magnetic materials (and to other uniaxial crystals if the anisotropy in the basal plane is small).

### 3.1 Ferromagnet

We take a plate of an orthorhombic ferromagnet bounded by the planes $y = \pm d_y/2$, and place it in a magnetic field $\mathbf{H} \parallel \mathbf{x}$. According to Eqns (2.2)–(2.5), the thermodynamic potential density is

$$F = \frac{1}{2} A'(\nabla_k \mathbf{m})^2 + (K_y m_y^{*2} + K_z m_z^{*2}) + B_{iklm} m_i^* m_k^* \mathcal{E}_{lm} + \frac{1}{2} c_{iklm} \mathcal{E}_{ik} \mathcal{E}_{lm} - H_x M_x - \frac{1}{2} \mathbf{H}_D \cdot \mathbf{M}\,, \tag{3.1}$$

where we have ignored the terms related to the anisotropy constant $K^{(2)}$ and the nonuniform magnetostriction constant $G$, which have no significant effect on the results.

Next we study the stability of the homogeneous ground state of a ferromagnet, in which $\mathbf{m}_0 = \mathbf{m}_0^* \parallel \mathbf{H} \parallel \mathbf{x}$ and $\mathcal{E} = \mathcal{E}_0$, where the spontaneous strain tensor $\mathcal{E}_0$ is determined from the condition that $\partial F(\mathbf{m} = \mathbf{m}_0)/\partial \mathcal{E}_{ik} = 0$. Substituting $\mathcal{E} = \mathcal{E}_0 + \Delta\mathcal{E}$ and $\mathbf{m}^* = \mathbf{m}_0 + \Delta\mathbf{m}^*$ into (3.1), we arrive at the following expression for the thermodynamic potential density in the harmonic approximation in $\Delta\mathbf{m}^*$ and $\partial u_i/\partial x_k$:

$$F = F_0 + \frac{1}{2}\Big\{ A'(\nabla_k \mathbf{m})^2 + \sum_{\alpha=y,z} \big[\tilde{K}_\alpha (m_\alpha - \omega_{\alpha x})^2 + MHm_\alpha^2 + 4B_{\alpha x \alpha x}(m_\alpha - \omega_{\alpha x}) e_{\alpha x}\big] - \mathbf{M} \cdot \mathbf{H}_D + c_{iklm} e_{ik} e_{lm} \Big\}\,, \tag{3.2}$$

where $F_0$ is the ground-state thermodynamic potential density,

$$\Delta\mathcal{E}_{ik} = e_{ik} + \frac{1}{2}\big[\mathcal{E}_0 e + e\mathcal{E}_0 + \mathcal{E}_0\omega - \omega\mathcal{E}_0\big]_{ik} + \frac{1}{2}\big[e^2 - \omega^2 + e\omega - \omega e\big]_{ik}\,,$$

$$\Delta m_y^* = m_y - \omega_{yx}\,, \qquad \Delta m_z^* = m_z - \omega_{zx}\,, \tag{3.3}$$

$$\Delta m_x^* = -\frac{1}{2}(m_y^2 + m_z^2 + \omega_{yx}^2 + \omega_{zx}^2) + m_y\omega_{yx} + m_z\omega_{zx}\,,$$

and $\tilde{K}_\alpha$ is the effective anisotropy constant, which takes into account spontaneous deformations (e.g., for crystals that have isotropic elastic and magnetoelastic properties, we have $\tilde{K}_\alpha = K_\alpha + B_{44}^2/c_{44}$).

The effect of the dipole interaction and nonuniform exchange on the final results will be discussed later.

In the frequency range of elastic waves, $\omega \ll \omega_s$ (here $\omega_s$ is the spin wave frequency at $k \to 0$), the magnetic subsystem has time to adjust itself to the elastic subsystem, so that its effect on the propagation of an elastic wave reduces to the renormalization of the static elastic constants of the crystal. Using the condition $\delta F/\delta m_\alpha = 0$, we can express the $m_\alpha$ in

terms of the distortion tensor components $u_{i,k}$. The result is

$$F = \frac{1}{2}\left[\sum_{i,k=x,y,z} c_{ik}e_{ii}e_{kk} + \sum_{\alpha=y,z}\left(c_1^{(\alpha)}u_{\alpha,x}^2 + c_2^{(\alpha)}u_{x,\alpha}^2 + 2c_3^{(\alpha)}u_{\alpha,x}u_{x,\alpha}\right) + 4c_{44}e_{yz}^2\right], \tag{3.4}$$

where

$$c_{1,2}^{(\alpha)} = c_{\alpha x\alpha x} + \frac{\tilde{K}_\alpha}{4} \mp B_{\alpha x\alpha x} - \left(B_{\alpha x\alpha x} \mp \frac{\tilde{K}_\alpha}{2}\right)^2 \frac{1}{HM + \tilde{K}_\alpha},$$

$$c_3^{(\alpha)} = c_{\alpha x\alpha x} - \frac{\tilde{K}_\alpha}{4} - \left(B_{\alpha x\alpha x}^2 - \frac{\tilde{K}_\alpha^2}{4}\right)\frac{1}{HM + \tilde{K}_\alpha}$$

are the effective elastic constants.

Below, we give the results for Rayleigh and Lamb ME waves propagating along the $x$ axis [113].

In the short-wavelength approximation ($kd_y \gg 1$), we arrive at a cubic equation for the spectrum of Rayleigh waves

$$(1-\varepsilon)\eta^3 - \left[2D_{12} + c_1^{(y)} - \varepsilon(2D_y + c_{11})\right]\eta^2 + \left[(D_{12} + c_1^{(y)})^2 - \varepsilon(D_y + c_{11})^2 - (c_1^{(y)2} - \varepsilon c_{11}^2)\right]\eta - (c_1^{(y)}D_{12}^2 - \varepsilon c_{11}D_y^2) = 0, \tag{3.5}$$

where

$$D_{ik} = c_{ii} - \frac{c_{ik}^2}{c_{kk}}, \qquad D_\alpha = c_1^{(\alpha)} - \frac{c_3^{(\alpha)2}}{c_2^{(\alpha)}} \qquad (\alpha = x, y),$$

$$\eta = \frac{\rho\omega^2}{k^2}, \qquad \varepsilon = \frac{c_2^{(y)}}{c_{22}}.$$

In highly anisotropic crystals, in which the interlayer interaction is much weaker than the intralayer ($c_{11} \gg c_{22}, c_{12}, c_i^{(y)}$), the dispersion law for the Rayleigh wave becomes simpler:

$$\rho\omega^2 = k^2\left(c_1^{(y)} - \frac{c_3^{(y)4}}{c_2^{(y)}c_{11}c_{22}}\right). \tag{3.6}$$

In the long-wavelength approximation ($kd_y \ll 1$), the dispersion law for the lowest-frequency Lamb waves can be written as

$$\rho\omega_1^2 = k^2 D_{12} \quad \text{(longitudinal mode)}, \tag{3.7}$$

$$\rho\omega_2^2 = k^2 D_y + \frac{k^4 d_y^2 c_3^{(y)2} D_{12}}{12 c_2^{(y)2}} \quad \text{(flexural mode)}. \tag{3.8}$$

The dispersion equation for the flexural wave propagating in the plate's plane at an angle to the magnetic field assumes the following form:

$$\rho\omega^2 = D_y k_x^2 + \frac{d_y^2}{12}\left\{k_x^4 D_{12}\left(\frac{c_3^{(y)}}{c_2^{(y)}}\right)^2 + k_z^4 D_{32} + k_z^2 k_x^2\left[2\left(c_{12}\left(1 - \frac{c_{23}}{c_{22}}\right) + c_3^{(2)}\right)\frac{c_3^{(y)}}{c_2^{(y)}} + c_1^{(z)} + c_2^{(z)}\left(\frac{c_3^{(y)}}{c_2^{(y)}}\right)^2\right]\right\}. \tag{3.9}$$

In accord with the results of Bar'yakhtar et al. [102], the presence of a magnetic field renders the plate a transverse rigidity. For this reason, the dispersion law for the flexural wave propagating at an angle $\varphi \neq \pi/2$ to the magnetic field is similar to that of a sound wave. The speed of propagation of this wave is

$$v_x = \left(\frac{D_y}{\rho}\right)^{1/2} = \left\{\frac{HMK_y^*}{\rho}\left[K_y^* + HM\left(1 - \left(\frac{K_y^*}{4} + B_{66}\right)\frac{1}{c_{66}}\right)\right]^{-1}\right\}^{1/2}, \tag{3.10}$$

where $K_y^* = \tilde{K}_y - B_{66}^2/c_{66}$.

Thus, by orienting the magnetic moments, an external magnetic field impedes the local rotation of the magnetic anisotropy axis upon the propagation of a flexural wave. Let us estimate the transverse rigidity of the given wave emerging as a result of this. Assuming that in a highly anisotropic magnetic material $K_y^* \approx 10^6 - 10^8$ erg cm$^{-3}$, $\rho \approx 5$ g cm$^{-3}$, and $H \gg K_y^*/M$, we find that $v_x \approx 10^3 - 10^4$ cm s$^{-1}$, which is 0.01–0.1 of the speed of sound in the crystal due to the symmetric components of the distortion tensor.

Now, we write the dispersion relation for the high-frequency Lamb waves in the long-wavelength approximation

$$\rho\omega_{\pm,p,n}^2 = \pi^2 n_{\pm,p}^2 d_y^{-2}\varepsilon_p + f_p^{\pm}k^2, \tag{3.11}$$

where $\omega_{\pm,p,n}$ are the frequencies of the symmetric and antisymmetric waves, respectively; $n_{\pm,p} = 2n - 1/2 \pm (-1)^p/2$, $p = 1, 2$ for the longitudinal and transverse waves, $n = 1, 2, \ldots$, $\varepsilon_1 = c_{22}$, $\varepsilon_2 = c_2^{(y)}$, and $f_p^{\pm}$ are functions of $c_{ik}$ and $c_i^{(\alpha)}$.

For the transverse wave polarized in the plate's plane, the dispersion law with $\mathbf{k} \parallel \mathbf{x}$ has the form

$$\rho\omega^2 = c_1^{(z)}k^2. \tag{3.12}$$

But if the plate's size $d_z$ is limited ($d_z \gg d_y$), the plate can be regarded as a rod with a rectangular cross section with sizes $d_y$ and $d_z$. When $k_x \ll d_z^{-1}$, the laws of dispersion for the longitudinal and flexural waves propagating along the rod can be written as

$$\rho\omega^2 = D_l k_x^2 \quad \text{(longitudinal mode)}, \tag{3.13}$$

$$\rho\omega^2 = D_y k_x^2 + \frac{d_y^2 k_x^4 D_l}{12} \quad \text{(flexural mode, polarized in the } xy \text{ plane)}, \tag{3.14}$$

$$\rho\omega^2 = D_z k_y^2 + \frac{d_z^2 k_x^4 D_l}{12} \quad \text{(flexural mode, polarized in the } xz \text{ plane)}, \tag{3.15}$$

where $D_l = c_{22} - 2c_{23}^2/(c_{22} + c_{23})$ at $c_{11} = c_{22}$ and $c_{12} = c_{23} = c_{31}$.

Let us assume that the anisotropy constants $K_i$, the magnetostriction constants $B_{iklm}$, and the elastic constants $c_{iklm}$ depend on the temperature $T$. Then the symmetric phase ($\mathbf{m} \parallel \mathbf{x}$, $u_{i,k} = 0$) becomes unstable when the square of the speed of propagation of one of the above modes vanishes on variations of the magnetic field. The square of the speed of propagation of the longitudinal wave in the plate [see

Eqn (3.7)] is positive for $D_{12}(T) > 0$. At $D_{12}(T) = 0$, the symmetric phase loses its stability with respect to the emergence of longitudinal displacements $u_x(x)$. The square of the speed of propagation of the flexural mode [see Eqn (3.8)] is positive for $D_y(T, H) > 0$. At $D_y(T, H) = 0$ the given phase loses its stability with respect to the emergence of transverse displacements $u_y(x, z)$ and, hence, of the plate flexure. In the absence of a dipole interaction $\mathbf{m} \parallel \mathbf{x}$, we have $u_{y,x} \neq 0$ and $u_{y,z} \neq 0$ (dissymmetric phase). As Eqn (3.10) implies, there are two cases where the condition $D_y(T, H) = 0$ is realized: when either the field changes sign ($H = 0$) or the anisotropy constant changes sign $\left[K_y^*(T) = 0\right]$. A portion of the phase diagram in the $HH_{\mathrm{A}}^{(y)}$ plane for the symmetric phase is depicted in Fig. 3, where $H_{\mathrm{A}}^{(y)} = K_y^*/M$.

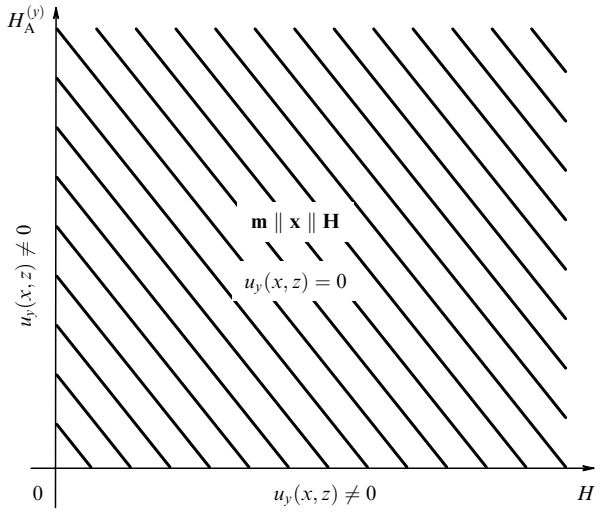


**Figure 3.** Portion of the phase diagram of a ferromagnetic plate constructed with allowance for the antisymmetric components of the distortion tensor for the symmetric phase $\mathbf{m} \parallel \mathbf{x} \parallel \mathbf{H}$, $u_y(x, z) = 0$ (the stability region is hatched).

On the lines of critical points ($H = 0$ and $H_{\mathrm{A}}^{(y)} = 0$), the speed of propagation of the Rayleigh wave [see Eqn (3.6)] remains finite (i.e., it does not vanish)

$$\tilde{s}_{\mathrm{R}} \simeq s_{\mathrm{t}}(1 - \zeta_6)^{1/2} \ll s_{\mathrm{R}} \,, \tag{3.16}$$

where $s_{\mathrm{t}} = (c_{66}/\rho)^{1/2}$, $\zeta_6 = H_{\mathrm{me6}}/(H_{\mathrm{me6}} + H + H_{\mathrm{A}}^{(y)})$, $H_{\mathrm{me6}} = B_{66}^2/(c_{66}M)$, and $s_{\mathrm{R}}$ is the speed of propagation of the Rayleigh wave far from an OPT. In this case the set of frequencies of transverse Lamb waves, $\omega_{\pm,2,n}$, is also finite:

$$\omega_{\pm,2,n}(k = 0) = \frac{\pi n_{\pm,2}}{d_y}\left(\frac{c_2^{(y)}}{\rho}\right)^{1/2} \simeq \frac{\pi n_{\pm,2}}{d_y}\, s_{\mathrm{t}}(1 - \zeta_6)^{1/2} \,. \tag{3.17}$$

At the triple point $H = H_{\mathrm{A}}^{(y)} = 0$, the speed of propagation of the Rayleigh wave, Eqn (3.16), that of the flexural wave, Eqn (3.10), and the set of the critical frequencies $\omega_{\pm,2,n}$ of the longitudinal Lamb waves, Eqn (3.17), vanish, so that there is an OPT into a phase with $m_y \neq 0$ and $u_y(x, z) \neq 0$. Note that as we get closer to the triple point, the depth $\Lambda$ of penetration of the Rayleigh wave into the crystal grows:

$$\Lambda = \frac{2\pi D_{12}^{3/2}}{\rho^{1/2}\omega c_{66}(1 - \zeta_6)} \tag{3.18}$$

and the wave's polarization approaches that of a transverse wave.

To calculate the attenuation of these surface waves, we do the following change of variables in Eqns (3.5)–(3.9): $H \to H - \mathrm{i}r\omega/g$ and $c \to c - \mathrm{i}\eta$. The attenuation coefficient is defined as the ratio of the imaginary and real parts of the complex-valued wave vector $k = k' + \mathrm{i}k''$:

$$\Gamma = \frac{k''}{k'} = \frac{\lambda}{2\pi\delta} \,, \tag{3.19}$$

where $\lambda = 2\pi/k$ is the wavelength, and $\delta = 1/k''$ is the effective attenuation length. For bulk and Rayleigh waves, we have

$$\Gamma = \frac{\omega}{2(1 - \zeta_6)}\left(\frac{\eta_{66}}{c_{66}} + \frac{\eta\zeta_6^2}{\omega_{\mathrm{me6}}}\right) ; \tag{3.20}$$

for flexural waves,

$$\Gamma_y = \frac{\omega}{2(H_{\mathrm{A}}^{(y)} + H)}\left(\frac{\eta_{66}}{c_{66}}\,\frac{HH_{\mathrm{me}}}{H_{\mathrm{A}}^{(y)}} + \frac{rH_{\mathrm{A}}^{(y)}}{gH}\right) . \tag{3.21}$$

As in the case of an unbounded medium, the attenuation coefficient of the surface wave grows as an OPT point is approached and attains its maximum at the transition point.

If the specimen is a rod, the symmetric phase loses stability with respect to the emergence of longitudinal and flexural (in the $xy$ and $xz$ planes) deformations [see Eqns (3.13)–(3.15)] when $D_1(T, H)$ and $D_{y,z}(T, H)$ change sign, respectively.

The fact that a magnetic field breaks the rotational symmetry of a magnetic material greatly affects the spectrum of the elastic waves and the phase diagram. Indeed, if we ignore the effects caused by the antisymmetric part of the distortion tensor, we can use the standard calculation methods [12, 14] to write the effective elastic constants as follows:

$$c_1^{(\alpha)} = c_2^{(\alpha)} = c_3^{(\alpha)} = c_{\alpha x \alpha x}\,\frac{H + H_{\mathrm{A}}^{(\alpha)}}{H + H_{\mathrm{A}}^{(\alpha)} + H_{\mathrm{me}}} \equiv c_\alpha^* \,, \qquad D_\alpha = 0 \,, \tag{3.22}$$

where $\alpha = y, z$, and $H_{\mathrm{A}}^{(z)} = K_z^*/M = (\tilde{K}_z - B_{55}^2/c_{55})/M$.

As $k \to 0$, the flexural-mode speeds vanish both for the case of a plate [Eqn (3.8)] and for the case of a rod (Eqs. (3.14) and (3.15)). In a plate, the Rayleigh-wave speed is

$$v = \left[\frac{c_y^*}{\rho}\left(1 - \frac{c_y^{*2}}{c_{11}c_{12}}\right)\right]^{1/2}$$

[see Eqn (3.6)], while the set of critical frequencies

$$\omega_{\pm,2,n} = \frac{\pi n_{\pm,2}}{d_y}\left(\frac{c_y^*}{\rho}\right)^{1/2}$$

[see Eqn (3.11)] vanishes on the line $H + H_{\mathrm{A}}^{(y)} = 0$ in the $(H, H_{\mathrm{A}}^{(y)})$ phase diagram (the straight $AB$ line in Fig. 4). On the segment $OA$ of this line, the symmetric phase $\mathbf{m} \parallel \mathbf{x}$, $u_{y,x} = 0$ (for $H_{\mathrm{A}}^{(y)} \geqslant -H$) loses its stability against transition to the angular phase $m_y \neq 0$, $u_y \neq 0$. On the straight line $OB$, the symmetric phase $\mathbf{m} \uparrow\uparrow \mathbf{x}$, $u_{y,x} = 0$ loses its stability against transition to the phase in which $\mathbf{m} \uparrow\downarrow \mathbf{x}$, $u_{y,x} = 0$. For $H_{\mathrm{A}}^{(y)} > 0$, in the interval $-H_{\mathrm{A}}^{(y)} < H < 0$ of field strengths, the state $\mathbf{m} \uparrow\uparrow \mathbf{x} \uparrow\downarrow \mathbf{H}$, $u_{y,x} = 0$ is metastable, and the straight line $H = 0$ is the line of OPTs between the states $\mathbf{m} \uparrow\uparrow \mathbf{x}$, $u_{y,x} = 0$

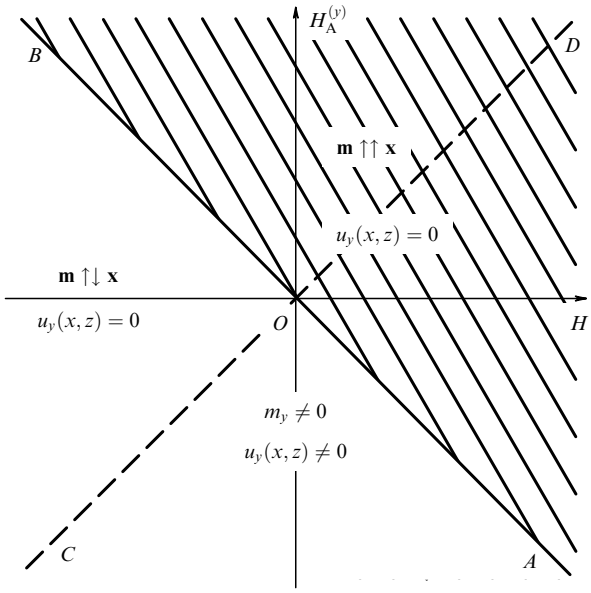


**Figure 4.** Phase diagram of a ferromagnetic plate constructed without allowance for the antisymmetric components of the distortion tensor. The region of stability of the symmetric phase $\mathbf{m} \uparrow\uparrow \mathbf{x}$, $u_y(x,z) = 0$ is hatched; the region of stability of the antisymmetric phase $\mathbf{m} \uparrow\downarrow \mathbf{x}$, $u_y(x,z) = 0$ lies above the $CD$ line; and the angular phase $m_y \neq 0$, $u_y(x,z) \neq 0$ is stable in the region $AOC$.

and $\mathbf{m} \uparrow\downarrow \mathbf{x}$, $u_{y,x} = 0$. The straight line $OA$ is the line of second-order OPTs.

Comparing these results with those mentioned earlier, we conclude that the violation of rotational invariance in the presence of a magnetic field leads to the following effects [113]: one of the flexural modes, (3.8), (3.14), or (3.15), becomes the soft acoustic mode; (2) the symmetric phase ($\mathbf{m} \parallel \mathbf{x}$, $u_{\alpha,x} = 0$) remains stable in the quadrant $H > 0$, $H_A^{(\alpha)} > 0$ of the $(H, H_A^{(\alpha)})$ phase diagram in Fig. 3. But if we ignore the effects of the antisymmetric part of the distortion tensor, the set of the critical modes $\omega_{\pm,2,n}$ and the Rayleigh wave are the soft acoustic modes, and the symmetric phase remains stable toward small perturbations in the half-plane $H + H_A^{(\alpha)} > 0$ of the $(H, H_A^{(\alpha)})$ phase diagram in Fig. 4.

Note that the investigated phase transition, accompanied by the emergence of transverse displacements $u_y(x,z)$, is characterized by the presence of a soft flexural mode, which leads to anomalously large fluctuations.

As the plate becomes thicker ($d_y$ grows), the wave-vector range

$$\Delta k \sim \frac{1}{d_y}\left(\frac{D_y}{D_{12}}\right)^{1/2}$$

in which anomalous dispersion manifests itself (i.e., the law of dispersion of the flexural wave is typical of sound waves) narrows, so that in the limit $d_y \to \infty$ we have $\Delta k \to 0$. When we are dealing with a massive specimen at $H = 0$, the shear bulk mode is the soft mode [12, 14].

Allowing for nonuniform exchange leads to dispersion in the elastic constants $c_i^{(\alpha)}$ in (3.4). Since for flexural vibrations of the plate the distribution of magnetization along the normal to the surface of the bent film can be assumed uniform, we write the dipole energy density in (3.2) in the form $2\pi M^2 m_x^{*2}$ [102]. Hence, when we allow for the effect of the dipole interaction on the spectrum of flexural vibrations, in Eqns (3.8)–(3.10) we must replace $K_y$ with $K_y + 4\pi M^2$. Figure 5 depicts the magnetization distribution in a plate in the dissymmetric phase for $H_A^{(y)} \gg 4\pi M$ and $H < 0$ or for $H_A^{(y)} + 4\pi M < 0$ and $H \gg 4\pi M$ (i.e., in situations where the domain structure is suppressed). The direction of the magnetization vector coincides with that of the internal field $\mathbf{H}_{\text{in}} = \mathbf{H} + \mathbf{H}_{\text{D}}$, where $\mathbf{H}_{\text{D}}$ is the demagnetizing field along the normal to the surface of the film. Since the directions of the vector $\mathbf{H}_{\text{D}}$ on the right and left sides of the axial line $YY$, on which $H_{\text{D}} = 0$ and $\mathbf{M} \parallel \mathbf{H}$, are different, the plate in the dissymmetric phase consists of two domains with different directions of magnetization. At $H_A^{(y)} \cong 4\pi M$ and $H < 0$ or at $H_A^{(y)} + 4\pi M < 0$ and $H \cong 4\pi M$, the dipole interaction may lead to the formation of a domain structure in the dissymmetric phase. The ways in which such a structure can emerges merit a special study.

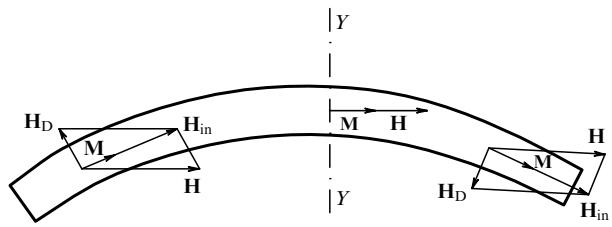


**Figure 5.** Distribution of magnetization in a plate in the dissymmetric phase (schematic).

There is also another way in which a system of domains may form near an OPT. If a longitudinal sound wave is propagating along a crystallographic axis with $H_A^{(\alpha)}$ close to zero, the emerging compression and stretching of the magnetic material due to magnetostriction lead to a periodic modulation of $K_\alpha^*$ [117]. Then, for $\tau \ll \tilde{T}$, where $\tau$ is the relaxation time of the elastic subsystem and $\tilde{T}$ is the period of the sound wave, the plate will bend in the regions where $K_\alpha^* < 0$.

### 3.2 Antiferromagnet

Let us place a plate of thickness $d_y$ of an orthorhombic antiferromagnet with weak ferromagnetism in a magnetic field $\mathbf{H} \parallel \mathbf{x}$. The thermodynamic potential density is given by Eqns (2.2), (2.4), (2.15), and (2.16). In the expression for $F_{\text{m}}$, we limit ourselves to the following representation for the anisotropy energy and the Dzyaloshinskiĭ invariant:

$$\frac{1}{2}(K_z l_z^{*2} + K_x l_x^{*2}) - (D_1 l_x^* m_y^* + D_2 l_y^* m_x^*)\,.$$

To simplify matters, we assume that $K_z \gg K_x$ (this corresponds to an easy-plane antiferromagnet with low anisotropy in the basal plane $xy$). We competely neglect the in-plane anisotropy in the elastic and ME energies. For moderate fields, we ignore the first and third terms on the right-hand side of expression (2.16) for the ME energy. In this approximation, the elastic and ME energies can be described by Eqns (2.4) and (2.16) with the following components being nonzero: $c_{11} = c_{22}$, $c_{33}$, $c_{12} = c_{21}$, $c_{13} = c_{23} = c_{31} = c_{32}$, $c_{44} = c_{55}$, $c_{66}$ and $B_{11} = B_{22}$, $B_{33}$, $B_{12} = B_{21}$, $B_{44} = B_{55}$; and $B_{66}$.

When our antiferromagnet is in its ground state, $\mathbf{l}_0 \parallel \mathbf{y}$ and $\mathbf{m}_0 \parallel \mathbf{x}$, while the spontaneous deformations are determined

by the conditions

$$\frac{\partial F(\mathbf{m}_0, \mathbf{l}_0)}{\partial \mathcal{E}_{ik}} = 0\,,$$

where $m_0 = (2M_0H + D_2)/E$ and $l_0 = \sqrt{1 - m_0^2} \sim 1$. In the harmonic approximation (in the small deviations of $\mathbf{l}$, $\mathbf{m}$, and $u_{ik}$ from the ground state), the thermodynamic potential density is

$$F = \frac{E}{2}(m_y^2 + m_z^2 + 2m_0\Delta_1) + \frac{1}{2}\tilde{K}_z(l_z - \omega_{zy})^2 + \frac{1}{2}\tilde{K}_x(l_x - \omega_{xy})^2 - 2M_0H\Delta_1 - D_1 l_x m_y - D_2\Delta_2 + 2B_{66}(l_x - \omega_{xy})e_{xy} + 2B_{44}(l_z - \omega_{zy})e_{zy} + \frac{1}{2}c_{iklm}e_{ik}e_{lm}\,. \tag{3.23}$$

Here

$$\Delta_1 \simeq -\left[2M_0Hl_x^2 + (D_1 + D_2)l_x(l_x - \omega_{xy}) + D_2\left(\frac{l_x^2 + l_y^2}{2} - \omega_{xy}l_x - \omega_{zy}l_z - \frac{\omega_{xy}^2 + \omega_{zy}^2}{2}\right)\right]\frac{1}{E}\,,$$

$$\Delta_2 \simeq \Delta_1 - 2\omega_{xy}m_y + m_0\omega_{zy}l_z - \omega_{xz}m_z - \frac{m_0(2\omega_{xy}^2 + \omega_{xz}^2 + \omega_{zy}^2)}{2}\,,$$

$$m_y = -m_0 l_x\,, \qquad m_z = -\frac{D_2\omega_{xz}}{E}\,.$$

For the effective anisotropy constants $\tilde{K}_\alpha$ we only write the expression for one constant:

$$\tilde{K}_x = K_x + \frac{2(B_{11} - B_{12})^2}{c_{11} - c_{12}}\,.$$

In the long-wavelength approximation $\omega \ll \omega_{1s} < \omega_{2s}$ (here $\omega_{1,2s}$ are the quasimagnon mode frequencies),

$$l_x = \frac{[\tilde{K}_x + 2(D_1 + D_2)m_0]\omega_{xy} - 2B_{66}e_{xy}}{2M_0Hm_0 + \tilde{K}_x + 2(D_1 + D_2)m_0}\,,$$

$$l_z = \frac{(\tilde{K}_z + D_2m_0)\omega_{zy} - 2B_{44}e_{zy}}{\tilde{K}_z + D_2m_0}\,.$$

As in the case of a ferromagnet, the elastic part of the thermodynamic potential is given by Eqn (3.4), where we must modify the effective elastic constants $c_i^{(\alpha)}$ $(\alpha = y, x)$ in the following manner: for $c_i^{(y)}$ we must perform the change of variables

$$\tilde{K}_y \to \tilde{K}_x + 2(D_1 + D_2)m_0\,, \qquad H \to 2Hm_0\,, \qquad M \to M_0\,, \tag{3.24}$$

and for $c_i^{(z)}$ we must put

$$c_1^{(z)} = c_2^{(z)} = c_{44} - \frac{HM_0D_2}{4E}\,, \qquad c_3^{(z)} = c_{44} + \frac{HM_0D_2}{4E}\,.$$

The results for Rayleigh and Lamb ME waves propagating along the $x$ axis of an antiferromagnetic plate are described by Eqns (3.5)–(3.12) and (3.16)–(3.22), in which, in addition to the change of variables (3.24), we must replace $K_y^*$ by

$$K_x^* = \tilde{K}_x + 2(D_1 + D_2)m_0 - \frac{B_{66}^2}{c_{66}}$$

[i.e., $H_A^{(y)}$ by $H_A^{(x)}$]. For instance, as in the case of a ferromagnet, a flexural wave, in the presence of a magnetic field, has a finite speed of propagation given by the following formula:

$$v_x = \left(\frac{D_y}{\rho}\right)^{1/2} = \left[\frac{2M_0Hm_0K_x^*}{\rho(K_x^* + 2M_0Hm_0)}\right]^{1/2}. \tag{3.25}$$

Actually, the specifics of the propagation of Rayleigh and Lamb ME waves in an antiferromagnetic plate are the same as in the case of a ferromagnetic plate considered above. First, at $H = 0$ and $H_A^{(x)} = 0$ the quadratic (flexural) dispersion law is replaced by the linear law for sound waves. Second, on the lines $H = 0$ and $H_A^{(x)} = 0$ of phase transitions from a symmetric $[\mathbf{m} \parallel \mathbf{x},\ \mathbf{l} \parallel \mathbf{y},\ u_y(x, z) = 0]$ to dissymmetric $[\mathbf{m} \parallel \mathbf{x}, \mathbf{l} \parallel \mathbf{y}, u_y(x, z) \neq 0]$ phases, it is the flexural mode that is soft (whose speed of propagation vanishes). As the phase transition lines are approached, the speed of propagation of the Rayleigh wave and the critical frequencies $\omega_{\pm 2,n}$ of the transverse Lamb waves decrease, remaining finite, however. Only at the triple point $H = H_A^{(x)} = 0$ do the Rayleigh wave and the transverse Lamb waves become soft, together with the flexural mode.

The attenuation of the surface ME waves under consideration has the same features as the attenuation in ferromagnets [see Eqns (3.20) and (3.21)].

### 3.3 Experimental studies of the propagation of Rayleigh magnetoelastic waves in magnetic materials

All experimental work in this area of research is centered on the propagation of Rayleigh ME waves. The specimens are plates of hematite and iron borate, which are easy-plane antiferromagnets. The dependence of the speed of sound on the magnitude and direction of a magnetic field was studied in [105–108]. Kukhtin et al. [105] found that for a Rayleigh wave propagating in the basal plane of a hematite crystal at right angles to the twofold axis ($\mathbf{k} \perp \mathbf{U}_2$) with $\mathbf{H} \parallel \mathbf{k}$, the coupling between the elastic and magnetic subsystems is at its minimum. The speed of propagation of such a wave is at its maximum, $s_R = 0.93(c_{44}/\rho)^{1/2}$, and is independent of the magnetic field strength $H$. If we rotate $\mathbf{H}$ in the basal plane by an angle $\varphi$ (Fig. 6), the ME coupling gets stronger and reaches its maximum value (and the speed its minimum value) at $\varphi = \pi/4$. The speed of propagation of the Rayleigh ME wave renormalized by the ME coupling, $\tilde{s}_R$, can be found by solving the following equation:

$$\tilde{s}_R^4\left(\tilde{s}_R^2 - \frac{c_{11}}{\rho}\right)\tilde{s}_t^2 = (\tilde{s}_R^2 - \tilde{s}_t^2)\left(\tilde{s}_R^2 - \frac{c_{11}}{\rho}\right)\left(\tilde{s}_R^2 - \frac{c_{11}}{\rho} + \frac{c_{13}^2}{\rho c_{33}}\right)^2, \tag{3.26}$$

where

$$\tilde{s}_t(H) = \left[\frac{c_{44}}{\rho}(1 - \zeta)\right]^{1/2}$$

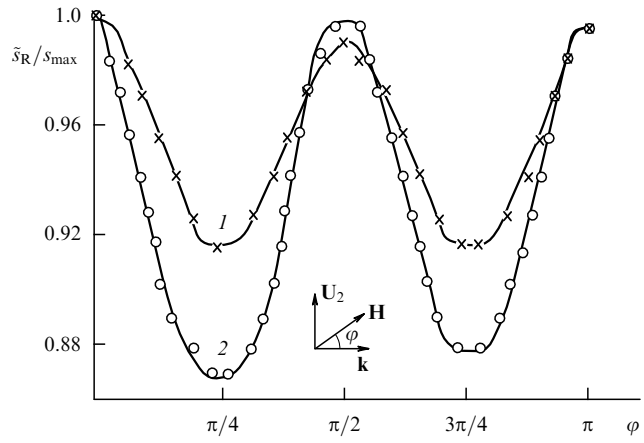


**Figure 6.** Dependence of the relative speed of propagation of Rayleigh waves, $\tilde{s}_R/s_{max}$, on the orientation of the magnetic field **H** in the basal plane of hematite [105]; curve *1* corresponds to $H = 2370$ Oe and curve *2*, to $H = 1300$ Oe.

is the speed of propagation of the shear bulk wave,

$$\zeta = \frac{g^2 H_E B_{14}^2}{M_0 c_{44} \omega_{s0}^2},$$

$$\omega_{s0} = g\left[H(H + H_D) + 2H_E H_{me}\right]^{1/2}$$

is the antiferromagnetic resonance frequency. The dependence of the speed of propagation of the Rayleigh wave on the orientation of **H** in the basal plane is depicted in Fig. 6 and on the magnitude of $H$ in Fig. 7 (the figures have been taken from [105]). The variation (decrease) in the speed of propagation of the Rayleigh wave (as the OPT point $H = 0$ is approached) is over 35%, and because of this such waves are important from practical viewpoint.

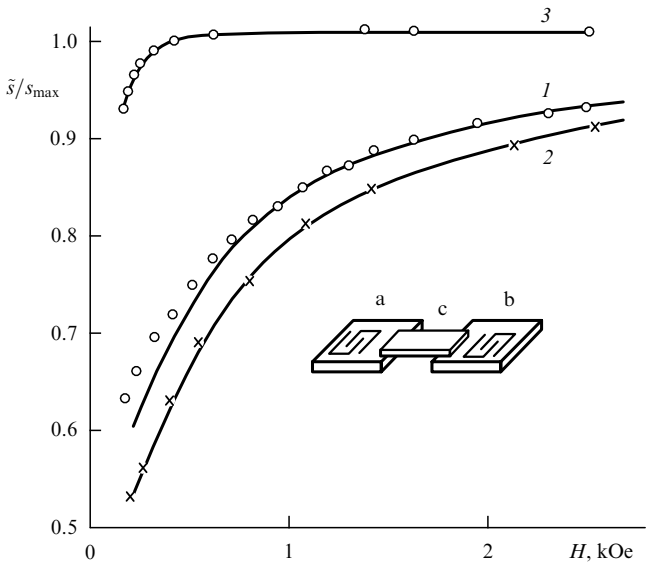


**Figure 7.** Dependence of the relative speeds of the Rayleigh ME waves, $\tilde{s}_R/s_{max}$ (curves *1* and *3*), and of the bulk transverse ME waves, $\tilde{s}_t/s_{max}$ (curves *2*), on the magnetic field strength $H$ in the basal plane of hematite [105]; curves *1* and *2* correspond to $\varphi = \pi/4$, and curve *3* to $\varphi = 0$; a and b are $LiNb_3$, and c is $\alpha$-$Fe_2O_3$.

The research done by Pol'skiĭ et al. [108] on the propagation of Rayleigh waves in crystals of gallium-substituted hematite ($\alpha$-$Fe_{2-x}Ga_xO_3$, $0 \leqslant x \leqslant 0.3$) with low Morin transition temperatures (as low as $-140\,^\circ$C) revealed that their $Q$ factors and their ability to transform the speed of propagation of surface ME waves are in no way inferior to pure hematite. Such materials could be used to manufacture acoustoelectronic devices operating stably at lower temperatures than hematite crystals would.

Second-harmonic generation for a Rayleigh ME wave in hematite was observed by Krasil'nikov et al. [109]. The most favorable geometry for observing this harmonic was found to be when $\mathbf{k} \parallel \mathbf{y}$ in a field **H** directed at an angle $\varphi = \pi/4$ to the twofold axis **x** in the $xy$ plane. At low levels of acoustic input power at the fundamental frequency $P_0$, the dependence of the second-harmonic acoustic power $P_2$ on $P_0$ is quadratic (Fig. 8). Figure 9 (both figures have been taken from [109])

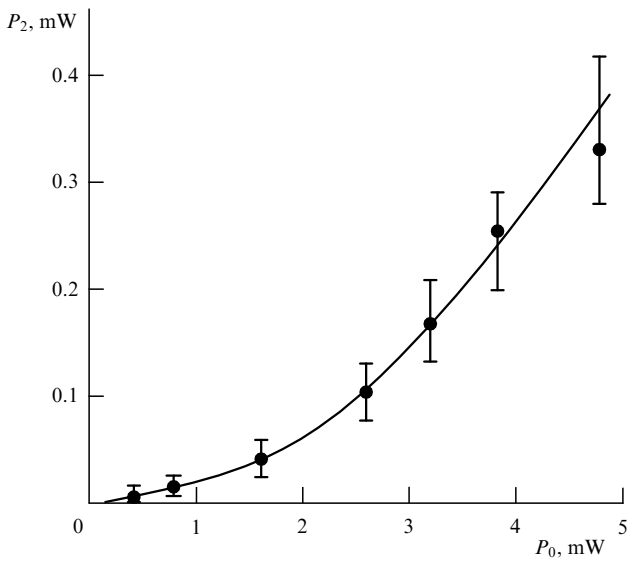


**Figure 8.** Dependence of the second-harmonic signal power $P_2$ on the fundamental-frequency signal power $P_0$ [109].

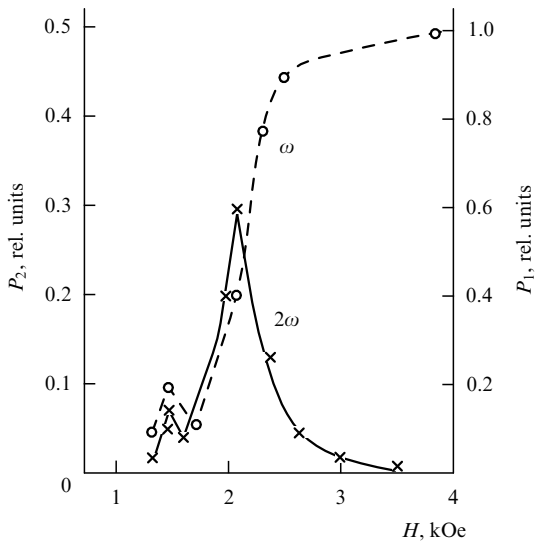


**Figure 9.** Dependence of the relative signal power for the fundamental frequency ($P_1$), and the second harmonic ($P_2$) on the magnetic field strength $H$ [109].

depicts the field dependence of $P_2$ and $P_1$, where $P_1$ is the first-harmonic power. If we start at a field of 4 kOe, $P_2$ grows with the field strength decreasing to 2 kOe, due to the increasing effective third-order elastic constants with decreasing field (as the OPT point is approached). Further growth is limited by the increase in attenuation and the deterioration of the conditions for excitation of the surface wave due to a decrease in the speed of propagation of the wave. The maximum fundamental to second-harmonic power conversion efficiency obtained by Krasil'nikov et al. [109] was 10–30% in a 2-kOe field. Qualitatively, these experimental data agree with the results of theoretical research done by Buchel'nikov et al. [112].

Another nonlinear ME effect, acoustic convolution in hematite, in which two oppositely traveling surface Rayleigh ME waves interact nonlinearly, was observed by Gubkin et al. [110] and Ermolov et al. [111]. Two geometries were used in the experiments. The first [110] coincided with that used by Krasil'nikov et al. [109], while in Ref. [111], oppositely directed surface waves propagated along the magnetic field: $\mathbf{k} \parallel \mathbf{H} \parallel \mathbf{x}$.

The nonlinear magnetization oscillations generated in the specimen at a double frequency (60 MHz) with a zero wave-vector difference, $\Delta k = 0$, were registered by the induction method [110]. Figure 10 depicts the dependence of the input signal amplitude on the field strength $H$. Qualitatively, the variation of the signal's amplitude (the convolution) as the OPT point is approached is the same as in the case of Rayleigh-wave second-harmonic generation.

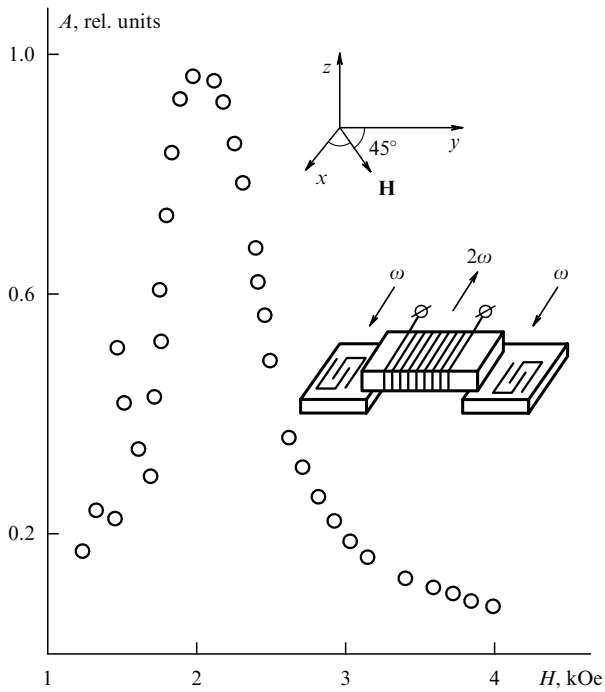


**Figure 10.** Dependence of the nonlinear-interaction output signal amplitude on the strength of a magnetic field directed at an angle of $\varphi = 45°$ to the $x$ and $y$ axes [110].

## 4. Shear surface magnetoacoustic waves (SSMAWs)

Let us now discuss the aspects of SSMAW propagation — waves caused by magnetostrictive and piezomagnetic mechanisms of ME coupling in various semi-infinite magnetic materials (ferro-, ferri-, and antiferromagnets). We also discuss the behavior of such waves in the vicinity of an OPT.

### 4.1 SSMAWs in ferromagnets

Suppose that a ferromagnet with its easy magnetization axis directed along the $z$ axis occupies the half-space $y > 0$ and is placed in a constant magnetic field $\mathbf{H} \parallel \mathbf{M} \parallel \mathbf{z}$. Parekh [84, 85] was the first to describe an SSMAW polarized along the $z$ axis and propagating along the $x$ axis along the surface of the crystal (Fig. 11).

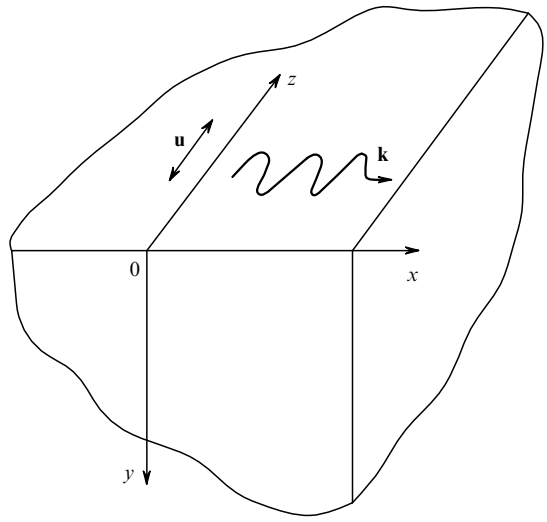


**Figure 11.** Geometry of the problem of SSMAW propagation in semi-infinite ferro- and antiferromagnets (here **u** is the polarization vector of the elastic wave).

For this problem the system of equations (2.7)–(2.9) describing the coupled oscillations of the magnetization and the lattice in the nonexchange approximation is

$$\mathrm{i}\omega m_x = \omega_0 m_y + g\,\frac{B_{44}}{M_0}\,\frac{\partial u_z}{\partial y} + \frac{\omega_M}{4\pi}\,\frac{\partial \Phi}{\partial y}\,,$$

$$\mathrm{i}\omega m_y = -\omega_0 m_x - g\,\frac{B_{44}}{M_0}\,\frac{\partial u_z}{\partial x} - \frac{\omega_M}{4\pi}\,\frac{\partial \Phi}{\partial x}\,,$$

$$-\rho\omega^2 u_z = c_{44}\nabla^2 u_z + B_{44}\left(\frac{\partial m_x}{\partial x} + \frac{\partial m_y}{\partial y}\right),$$

$$\nabla^2 \Phi = 4\pi\left(\frac{\partial m_x}{\partial x} + \frac{\partial m_y}{\partial y}\right), \tag{4.1}$$

where $\omega_0 = g(H + H_{\mathrm{A}} + H_{\mathrm{me4}})$, $\omega_M = 4\pi g M_0$, and $\mathbf{H}_{\mathrm{D}} = -M_0 \nabla \Phi$ ($\Phi$ is the dipole field potential).

We seek the solution of this system of equations in the form

$$m_{x,y}\,, \Phi^{(\mathrm{i})}, u_z \propto \exp\left[-\alpha_{\pm}|k|y + \mathrm{i}(kx - \omega t)\right],$$

$$\Phi^{(\mathrm{e})} \propto \exp\left[|k|y + \mathrm{i}(kx - \omega t)\right]. \tag{4.2}$$

The labels 'i' and 'e' imply that $\Phi$ refers to the regions where $y > 0$ and $y < 0$, respectively. The subscript on $\alpha_{\pm}$ reflects the fact that the wave propagates in the positive or negative directions along the $x$ axis.

Substituting this solution into (4.1), we arrive at the characteristic equation for $\alpha$, which determines the depth $\Lambda = (\alpha k)^{-1}$ of penetration of SSMAWs into the crystal:

$$(\alpha^2 - \alpha_{1\pm}^2)(\alpha^2 - \alpha_{2\pm}^2) = 0\,. \tag{4.3}$$

Here

$$\alpha_{1\pm} = 1\,, \tag{4.4}$$

$$\alpha_{2\pm}^2 = 1 - \frac{\omega^2 f(\omega)}{s_{\rm t}^2 k^2}\,, \tag{4.5}$$

$$f(\omega) = \left(1 - \frac{\omega_{\rm me4}\omega_0}{\omega_0\omega_B - \omega^2}\right)^{-1},$$

$$\omega_B = \omega_0 + \omega_M\,, \qquad \omega_{\rm me4} = gH_{\rm me4}\,. \tag{4.6}$$

To clarify the physical meaning of $f(\omega)$, we substitute $\mathrm{i}k_y$ for $k_y = \alpha_{2\pm}k$ in (4.5) (first multiplying both sides of (4.5) by $k^2 = k_x^2$). This leads to a dispersion equation for coupled bulk ME waves

$$(\omega^2 - s_{\rm t}^2\kappa^2)(\omega^2 - \omega_0\omega_B) - s_{\rm t}^2\kappa^2\omega_{\rm me4}\omega_0 = 0\,, \tag{4.7}$$

with $\kappa^2 = k_x^2 + k_y^2$. For small values of $\kappa$ this equation describes a bulk shear wave and a bulk spin wave, respectively, both modified by ME coupling:

$$\omega_1 = \frac{s_{\rm t}\kappa}{\left[f(\omega)\right]^{1/2}}\,, \qquad \omega_2 = \left(\omega_0\omega_B + \frac{s_{\rm t}^2\kappa^2\omega_{\rm me4}}{\omega_B}\right)^{1/2}. \tag{4.8}$$

Thus, the coefficient $\left[f(\omega)\right]^{-1/2}$ determines the variation of the speed of propagation of a bulk transverse sound wave and its dispersion.

The solution of system (4.1) for a Parekh surface wave has the form

$$u_z = A\exp\left(-\alpha_{2\pm}|k|y\right)\exp\left[\mathrm{i}(\sigma|k|x - \omega t)\right],$$

$$\Phi^{(\rm i)} = -A\,\frac{B_{44}}{\mu M_0^2}\left[\frac{1-\mu+\sigma\chi}{1+\mu+\sigma\chi}\exp\left(-|k|y\right) + (\mu-1)\exp\left(-\alpha_{2\pm}|k|y\right)\right]\exp\left[\mathrm{i}(\sigma|k|x - \omega t)\right],$$

$$\Phi^{(\rm e)} = -A\,\frac{B_{44}}{\mu M_0^2}\,\frac{\mu-1+\sigma\chi}{1+\mu+\sigma\chi}\exp\left(|k|y\right)\exp\left[\mathrm{i}(\sigma|k|x - \omega t)\right], \tag{4.9}$$

where $A$ is the SSMAW amplitude, $\mu = 1 + \omega_M\omega_0/(\omega_0^2 - \omega^2)$, and $\chi = \omega_M\omega/(\omega_0^2 - \omega^2)$, $\sigma = k/|k| = \pm 1$ (the 'plus' corresponds to the propagation of the ME wave in the positive direction of the $x$ axis).

The boundary conditions (2.10)–(2.13) yield the following relationship:

$$\alpha_{2\pm} = \frac{\omega_{\rm me4}(\omega - \sigma\omega_+)(\omega + \sigma\omega_-)}{(\omega_{\rm DE} - \sigma\omega)\left[\omega^2 - \omega_0(\omega_B - \omega_{\rm me4})\right]}\,, \tag{4.10}$$

where $\omega_\pm = \left\{\left[\omega_0(\omega_B + \omega_M)\right]^{1/2} \pm \omega_0\right\}/2$, and $\omega_{\rm DE} = (\omega_0 + \omega_B)/2$ is the frequency of the Damon–Eshbach wave.

Substituting (4.10) into (4.5), we arrive at a dispersion equation for SSMAWs in the form

$$\frac{s_{\rm t}^2 k^2}{\omega^2} = \frac{f(\omega)}{1 - \alpha_{2\pm}^2}\,. \tag{4.11}$$

From (4.10) and (4.11) we see that the SSMAW is nonreciprocal and exists in the range of frequencies $\omega$ in which $\alpha_{2\pm} > 0$ and the right-hand side of (4.11) is positive, i.e., $0 < \alpha_{2\pm} < 1$.

The spectrum of coupled ME waves in a semi-infinite ferromagnet is depicted in Fig. 12 [84, 85]. The hatched sections correspond to regions where bulk ME waves can exist. Note that for real ferromagnets, such as YIG (yttrium iron garnet) crystals, the dispersion curves for SSMAWs lie very near the corresponding curves for bulk ME waves. Hence, to emphasize the features of the SSMAW spectrum, all scales in Fig. 12 have been distorted.

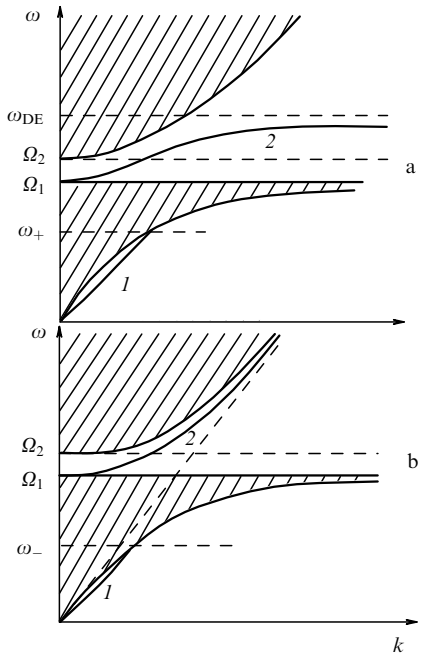


**Figure 12.** The SSMAW spectrum for $H \neq 0$: (a) $\sigma = 1$ and (b) $\sigma = -1$; curve *1* represents the lower SSMAW branch and curve *2* the upper SSMAW branch; the hatched sections correspond to the regions where bulk ME waves can exist; $\Omega_1 = \left[\omega_0(\omega_B - \omega_{\rm me4})\right]^{1/2}$, and $\Omega_2 = (\omega_0\omega_B)^{1/2}$ [64].

Without allowance for ME coupling ($H_{\rm me4} = 0$), the dispersion equation (4.11) describes three noninteracting waves: a Damon–Eshbach surface magnetostatic wave, a bulk magnetostatic wave, and a transverse bulk elastic wave with the following dispersion laws:

$$\omega = \frac{\omega_0 + \omega_B}{2}\,, \qquad \omega = \sqrt{\omega_0\omega_B}\,, \qquad \omega = \sqrt{\frac{c_{44}}{\rho}}\,. \tag{4.12}$$

At the point where the wave with $\mathbf{M} \parallel \mathbf{z}$ loses its stability at $H + H_{\rm A} = 0$, the frequency of the surface quasimagnon branch has a gap $\omega = \omega_{\rm me4} + \omega_M/2$. The speed of propagation of the quasiphonon branch decreases somewhat as this point is approached, but remains finite:

$$\tilde{s}_{\rm t} = \sqrt{\frac{\tilde{c}_{44}}{\rho}}\left[1 - \frac{\omega_{\rm me4}^2}{(\omega_M + \omega_{\rm me4})^2}\right], \tag{4.13}$$

where $\tilde{c}_{44} = c_{44}\left[1 - \omega_{\rm me4}/(\omega_M + \omega_{\rm me4})\right]$.

The spectrum of ME waves at the OPT point fixed by the condition $H + H_{\rm A}^{(y)} = 0$ can also be represented by Fig. 12

when the characteristic frequencies assume the following values:

$$\Omega_1^2 = \omega_{\mathrm{me4}}\omega_M\,, \qquad \Omega_2^2 = \omega_{\mathrm{me4}}(\omega_M + \omega_{\mathrm{me4}})\,,$$

$$\omega_\pm = \frac{1}{2}\left\{\left[\omega_{\mathrm{me4}}(2\omega_M + \omega_{\mathrm{me4}})\right]^{1/2} \pm \omega_{\mathrm{me4}}\right\},$$

$$\omega_{\mathrm{DE}} = \frac{\omega_M}{2} + \omega_{\mathrm{me4}}\,.$$

This result differs considerably from that obtained by Scott and Mills [64] and Parekh [84, 85]. Since these researchers ignored the ME gap in the spectrum of ME waves, they obtained $\Omega_1 = \Omega_2 = \omega_+ = \omega_- = 0$ at the OPT point. Allowing for the ME gap leads to a situation in which the given characteristic frequencies are finite, so that the fine structure of the spectrum of ME waves at the OPT point is conserved in the low-frequency range.

Note that the Parekh wave differs from the Gulyaev–Bluestein waves (GBWs) in that, first, it is nonreciprocal and, second, it is generated as a result of the resonant interaction of a bulk transverse elastic wave with a bulk magnetostatic wave and a Damon–Eshbach surface wave.

### 4.2 SSMAWs caused by the piezomagnetic effect in antiferromagnets

The piezomagnetic effect, predicted by Dzyaloshinskiĭ [114], was discovered experimentally by Borovik-Romanov [115] in two tetragonal antiferromagnets with easy-axis anisotropy ($\mathbf{L} \parallel \mathbf{z}$): $CoF_2$ and $MnF_2$. For such magnetic structures, a fraction of the free energy describing the piezomagnetic effect has the following form in the system of coordinates $x', y', z$ linked to the crystallographic axes [114, 116]:

$$F_{\mathrm{PM}} = -p_1(H_{\mathrm{D}x'}e_{y'z} + H_{\mathrm{D}y'}e_{zx'}) - p_2 H_{\mathrm{D}z}e_{x'y'}\,, \tag{4.14}$$

where $p_{1,2}$ are the components of the tensor of piezomagnetic constants.

Suppose that an SSMAW polarized along the $\mathbf{z}$ axis propagates in a tetragonal antiferromagnet in the (110) plane along axis $\mathbf{x}$ (see Fig. 11). Then, in a system of coordinates $x, y, z$ rotated with respect to the 'primed' system of coordinates through an angle of $\pi/4$ about the $\mathbf{z}$ axis, formula (4.14) becomes

$$F_{\mathrm{PM}} = -p_1(H_{\mathrm{D}x}e_{zx} - H_{\mathrm{D}y}e_{yz})\,. \tag{4.15}$$

The system of equations for the SSMAW is reduced to

$$\rho u_z = c_{44}\left(\frac{\partial^2 u_z}{\partial x^2} + \frac{\partial^2 u_z}{\partial y^2}\right) + \frac{p_1}{2}\left(\frac{\partial^2 \Phi^{(\mathrm{i})}}{\partial x^2} - \frac{\partial^2 \Phi^{(\mathrm{i})}}{\partial y^2}\right),$$

$$-2\pi p_1\left(\frac{\partial^2 u_z}{\partial x^2} - \frac{\partial^2 u_z}{\partial y^2}\right) + \mu\left(\frac{\partial^2 \Phi^{(\mathrm{i})}}{\partial x^2} + \frac{\partial^2 \Phi^{(\mathrm{i})}}{\partial y^2}\right) = 0\,,$$

$$\frac{\partial^2 \Phi^{(\mathrm{e})}}{\partial x^2} + \frac{\partial^2 \Phi^{(\mathrm{e})}}{\partial y^2} = 0\,, \tag{4.16}$$

where $\mu$ is the permeability of the antiferromagnet, $\mu = 1 + 16\pi M_0^2/E$.

We seek the solution of this system of equations in the form

$$u_z, \Phi^{(\mathrm{i})} \propto \exp\left[-\alpha k y + \mathrm{i}(kx - \omega t)\right],$$

$$\Phi^{(\mathrm{e})} \propto \exp\left[ky + \mathrm{i}(kx - \omega t)\right], \tag{4.17}$$

where $\alpha$ is a parameter characterizing the depth of the wave penetration into the material.

Substituting this solution into (4.16), we arrive at a characteristic equation for an SSMAW in the piezomagnet under consideration:

$$\left[\frac{s^2}{s_{\mathrm{t}}^2} + (\alpha^2 - 1)\right](\alpha^2 - 1) + \eta(\alpha^2 + 1)^2 = 0\,. \tag{4.18}$$

Here $s$ and $s_{\mathrm{t}}$ are the speeds of propagation of an SSMAW and a bulk transverse wave renormalized by ME coupling, respectively, and $\eta = \pi p_1^2/(\mu c_{44})$ is the magnetomechanical coupling constant (similar to the electromechanical coupling constant for piezoelectric crystals).

Note that the dispersion equation for SSMAWs caused by magnetostriction in ferro- and antiferromagnets differs from (4.18) in the sign in front of the unity in the last term. This fact considerably simplifies finding the roots of the dispersion equation for SSMAWs caused by magnetostriction. The resulting solution is identical to the solution for the GBWs in piezoelectric crystals. But in the case of SSMAWs considered here the solution of the dispersion equation (4.18) becomes more complicated because of the piezomagnetic effect, which naturally must lead to new results.

The system of equations (4.16) must be solved together with the boundary conditions (2.10)–(2.13), which in the case at hand can be written in a simpler form:

$$\sigma_{zy} = 0\,, \qquad B_y^{(\mathrm{i})} = -\frac{\partial \Phi^{(\mathrm{e})}}{\partial y}\,, \qquad \Phi^{(\mathrm{i})} = \Phi^{(\mathrm{e})} \quad \text{at} \quad y = 0\,. \tag{4.19}$$

To within a constant factor $A$, the solution of the system (4.16) can be written as follows

$$u_z = \left[C_1 \exp(-\alpha_1 k y) - C_2 \exp(-\alpha_2 k y)\right] A \exp\left[\mathrm{i}(kx - \omega t)\right],$$

$$\Phi^{(\mathrm{i})} = \frac{2\pi p_1}{\mu}\left[D_1 \exp(-\alpha_1 k y) - D_2 \exp(-\alpha_2 k y)\right] \times A \exp\left[\mathrm{i}(kx - \omega t)\right],$$

$$\Phi^{(\mathrm{e})} = \frac{2\pi p_1}{\mu}\left(D_1 - D_2\right) A \exp\left[ky + \mathrm{i}(kx - \omega t)\right]. \tag{4.20}$$

Here

$$C_i = -\frac{\alpha_i^2 - 1}{\alpha_i^2 + 1} D_i\,, \qquad D_i = \left(1 + \frac{2\mu\alpha_i}{\alpha_i^2 + 1}\right)^{-1}. \tag{4.21}$$

The dispersion equation has the form

$$\left(\frac{s}{s_{\mathrm{t}}}\right)^2 - 1 - \frac{\alpha_1}{\alpha_2}\left[1 + \mu(1 + \eta)(\alpha_1 + \alpha_2)\right] = 0\,. \tag{4.22}$$

The equation leads to the following expressions for the speed of propagation $s$ and the depth of penetration $\Lambda = (\alpha k)^{-1}$ of SSMAWs:

$$s \simeq s_{\mathrm{t}}\left(1 + \eta - \frac{\eta^2}{1 + \mu}\right),$$

$$\alpha_1 \simeq 1 - 2\eta\,, \qquad \alpha_2 \simeq \frac{\eta}{1 + \mu}\,. \tag{4.23}$$

In an approximation linear in the parameter $\eta$, we can write the following expressions for the constants $C_i$ and $D_i$:

$$C_1 = 2D_1\eta = \frac{2\eta}{1+\mu}\,, \qquad C_2 = D_2 = 1 - \frac{2\mu\eta}{1+\mu}\,. \qquad (4.24)$$

We see that in antiferromagnets, a SSMAW due to piezomagnetic effect is a purely shear wave propagating at a speed that is somewhat lower than that of the corresponding transverse bulk wave with ME renormalization [86–91] (just as a GBW is in all the known cases where it exists [45, 46]). But since the symmetry of the problem is different, the system of equations (4.16) and its solutions (4.20) differ substantially from the initial equations (4.1) and the solutions (4.9) describing magnetostriction-related SSMAWs in magnetic materials. The main difference is the pattern of the distribution of the elastic displacements and the variable magnetostatic field in the crystal. Schematically such a distribution for the SSMAW being considered is depicted in Fig. 13. For instance, in addition to having a long-range elastic-displacement component $u_z \propto \exp(-\alpha_2 ky)$ (just as in a GBW), the SSMAW under consideration (which propagates in the antiferromagnet) has a short-range component $u_z \propto \eta \exp(-\alpha_1 ky)$, which vanishes in the $\eta \to 0$ limit ('switching-off' of paramagnetism). In comparison to the well-known shear SAW, the long-range component of the wave we are interested in $\left[u_z, \Phi^{(\mathrm{i})} \propto \exp(-\alpha_2 ky)\right]$ does not penetrate the material so deep, provided that the electromechanical and magnetomechanical coupling constants of the materials being compared are close in value.

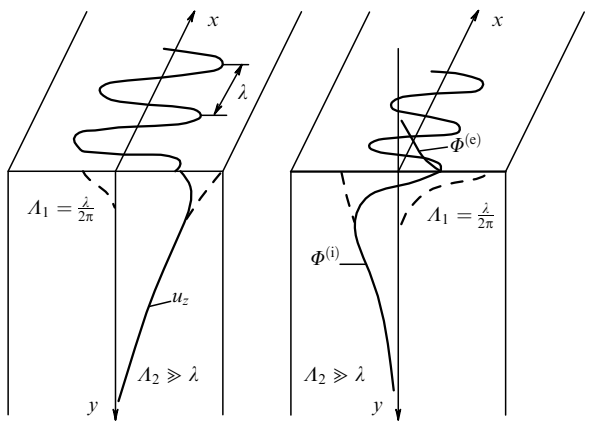


**Figure 13.** Distributions of the elastic ($u_z$) and magnetostatic ($\Phi^{(\mathrm{i})}$) oscillations in an SSMAW in an easy-axis tetragonal antiferromagnet, caused by the piezomagnetic effect. The dashed curves represent the distribution of partial SSMAW oscillations.

Note that the SSMAW we are examining here can also exist in hexagonal and cubic antiferromagnets. For instance, the results for SSMAWs due to piezomagnetic effect propagating in hexagonal nickel arsenide-type antiferromagnets (with an easy-plane anisotropy) are similar to those discussed above.

We also note that in all cases, as $\eta \to 0$, an SSMAW becomes transformed into a bulk transverse wave.

We believe that the antiferromagnetic $CoF_2$ is a material in which, apparently, one can observe the predicted SSMAW. Compared to other uniaxial crystals, this antiferromagnet has exhibited the highest piezomagnetic constants. Using Borovik-Romanov's results [115], we estimate the magnetomechanical coupling constant to be $\eta \sim 10^{-3}$, which is close to the values of electromechanical coupling constants of ordinary piezoelectric crystals [42]. But if we allow for the fact that Moriya [118] gives a value of $\eta$ larger than the value obtained in Ref. [115] by a factor of eight, the values of the piezomagnetic constants prove to be of the same order of magnitude as the values of piezoelectric constants in piezoelectric crystals. What will also facilitate experimental observation of the predicted waves is the fact that an SSMAW is always accompanied by a variable magnetostatic wave in the vacuum near the surface of the solid. Since in Ref. [115] the measurements were static, the effect we have just discussed may serve as a manifestation of a dynamic piezomagnetic interaction.

## 5. Conclusion

We have reviewed the results of theoretical and experimental studies of the propagation of ME waves in magnetic crystals with free surfaces near an OPT point. It is well known (e.g., see [119]) that an OPT is a particular case of a ferroelastic transition. A characteristic feature of such a transition is the linear relationship between the order parameter and macroscopic lattice deformations. Many features of a ferroelastic phase transition are of a general nature and are independent of the specific physical quantities that lead to the phase transition, i.e., are independent of the microscopic realization of the order parameter. In view of this, the ideas discussed in this review that refer to the nature of the soft mode defining the phase transition and to the effects emerging in the propagation of hybrid waves may prove useful in interpreting the theoretical and experimental results in the process of studying a broad class of ferroelastic-type magnetic phase transitions that take place in finite specimens. At present we can report positive examples of the utilization of these ideas. For instance, a number of new features of the propagation of Rayleigh waves in plates of ferroelectric ferroelastic materials in linear and nonlinear modes near ferroelastic phase transitions were first theoretically predicted [120] and then discovered in experiments [121–124]. Among these are the decrease of the speed of propagation of the Rayleigh wave; an increase of the depth of penetration of the waves into the crystal; and the nonlinear effects of frequency doubling and acoustic convolution. Analogies with magnetic systems have been widely used in building the theory of these phenomena. Effects associated with violation of the rotational invariance of the energy of an electrically polarized crystal with respect to its orientation in space in the presence of an electric field were studied by Bar'yakhtar et al. [125].

One should expect that effects associated with violation of the rotational invariance in a magnetic field most vividly manifest themselves in low-dimensional (layered and chain) magnetic materials [102]. The present authors proposed a new mechanism for low-temperature magnetostriction of such magnetic materials. Low-dimensional magnetic materials have a negative temperature coefficient of thermal expansion [126] because of a reduction of the longitudinal size of the crystal related to the generation of flexural vibrations. The amplitude of such vibrations increases with temperature. A magnetic field leads to the appearance of transverse rigidity in the flexural vibrations and to suppression of the amplitude of the vibrations, which restores the size of the crystal. Since this

mechanism is unrelated to changes in the interatomic distance. magnetostriction in such systems may be relatively large.

It must be noted that many ME effects discussed in this review are still awaiting experimental verification. For instance, the features of the spectrum of magnetoflexural waves and SSMAWs caused by magnetostriction and piezomagnetic effect have only been studied by theoreticians. An exciting experiment would be to study strong nonlinear effects near an OPT (solitons, shock waves, the formation of dynamic domain structures) — effects that have so far been studied mostly by theoretical methods [31, 127 – 133].

In conclusion, we would like to briefly discuss the difficulties that arise in interpreting the experimental data on the propagation of ME waves near an OPT. A number of factors concern discrepancies between the theoretical results and the experimental data. First, there are the magnetic and structural inhomogeneities in the specimens, including the domain structure of the specimens. In particular, if domains are formed as a result of an OPT, the phase and group velocities of ME waves with a finite wave-vector value $k = k_c$ [134, 135] (where $k_c$ is the reciprocal period of the emerging domain structure) vanish. ME wave scattering by magnetic and structural defects of the magnetic crystal leads to a stronger attenuation of these waves [38].

## References


1. Vonsovskiĭ S V *Magnetizm* (Magnetism) (Moscow: Nauka, 1971) [Translated into English (New York: Wiley, 1974)]
2. Turov E A, Irkhin Yu P *Fiz. Met. Metalloved.* **3** 15 (1956)
3. Akhiezer A I, Bar'yakhtar V G, Peletminskiĭ S V *Zh. Eksp. Teor. Fiz.* **35** 228 (1958) [*Sov. Phys. JETP* **8** 157 (1959)]
4. Kittel C *Phys. Rev.* **110** 836 (1958)
5. Peletminskiĭ S V *Zh. Eksp. Teor. Fiz.* **37** 452 (1959) [*Sov. Phys. JETP* **37** 321 (1960)]
6. Borovik-Romanov A S, in *Proc. 3rd Int. Conf. on Low Temperature Physics* (Prague, 1963) p. 86
7. Tasaki A, Iida S *J. Phys. Soc. Jpn.* **18** 1148 (1963)
8. Borovik-Romanov A S, Rudashevskiĭ E G *Zh. Eksp. Teor. Fiz.* **47** 2095 (1964) [*Sov. Phys. JETP* **20** 1407 (1965)]
9. Turov E A, Shavrov V G *Fiz. Tverd. Tela* (Leningrad) **7** 217 (1965) [*Sov. Phys. Solid State* **7** 166 (1965)]
10. Cooper B R, in *Magnetic Properties of Rare Earth Metals* (Ed. R J Elliot) (London, New York: Plenum Press, 1972) p. 17
11. Turov E A, Shavrov V G *Usp. Fiz. Nauk* **140** 429 (1983) [*Sov. Phys. Usp.* **26** 593 (1983)]
12. Dikshteĭn I E, Turov E A, Shavrov V G, in *Dinamicheskie i Kineticheskie Svoĭstva Magnetikov* (Dynamic and Kinetic Properties of Magnetic Substances) (Eds S V Vonsovskiĭ, E A Turov) (Moscow: Nauka, 1986) Ch. 3
13. Chow H, Keffer F *Phys. Rev. B* **7** 2028 (1973)
14. Dikshteĭn I E, Tarasenko V V, Shavrov V G *Zh. Eksp. Teor. Fiz.* **67** 816 (1974) [*Sov. Phys. JETP* **40** 404 (1975)]
15. Jensen J *J. Phys. C* **8** 2769 (1975)
16. Dikshteĭn I E, Tarasenko V V, Shavrov V G *Fiz. Tverd. Tela* (Leningrad) **19** 1107 (1977)
17. Ozhogin V I, Maximenkov P P *IEEE Trans. Magn.* **MAG-8** 645 (1972)
18. Shcheglov V I *Fiz. Tverd. Tela* (Leningrad) **14** 2180 (1972) [*Sov. Phys. Solid State* **14** 1889 (1973)]
19. Seavey M H *Solid State Commun.* **10** 219 (1972)
20. Maksimenkov P P, Ozhogin V I *Zh. Eksp. Teor. Fiz.* **65** 657 (1973) [*Sov. Phys. JETP* **38** 324 (1974)]
21. Berezhnov V V et al. *Radiotekh. Elektron.* **28** 376 (1983)
22. Jensen J, Palmer S B *J. Phys. C: Solid State Phys.* **12** 4573 (1979)
23. Gorodetsky G, Luthi B *Phys. Rev. B* **2** 3688 (1970)
24. Grishmanovskiĭ A N et al. *Fiz. Tverd. Tela* (Leningrad) **16** 1426 (1974) [*Sov. Phys. Solid State* **16** 916 (1974)]
25. Gorodetsky G, Shaft S, Wanklyn B M *Phys. Rev. B* **14** 2051 (1976)
26. Balbashov A M et al. *Fiz. Tverd. Tela* (Leningrad) **31** 279 (1989) [*Sov. Phys. Solid State* **31** 1259 (1989)]
27. Shapira Y *Phys. Rev.* **184** 589 (1969)
28. Buchel'nikov V D, Shavrov V G *Fiz. Met. Metalloved.* **68** 421 (1989)
29. Ozhogin V I, Preobrazhenskiĭ V L *Zh. Eksp. Teor. Fiz.* **73** 988 (1977) [*Sov. Phys. JETP* **46** 523 (1977)]
30. Ozhogin V I, Preobrazhenskiĭ V L *Usp. Fiz. Nauk* **155** 593 (1988) [*Sov. Phys. Usp.* **31** 713 (1988)]
31. Ozhogin V I, Preobrazhensky V L *J. Magn. Magn. Mater.* **100** 544 (1991)
32. Ozhogin V I, Lebedev A Yu, Yakubovskiĭ A Yu *Pis'ma Zh. Eksp. Teor. Fiz.* **27** 333 (1978) [*JETP Lett.* **27** 313 (1978)]
33. Dikshteĭn I E, Tarasenko V V *Fiz. Tverd. Tela* (Leningrad) **20** 2942 (1978) [*Sov. Phys. Solid State* **20** 1699 (1978)]
34. Evtikhiev N N et al. *Voprosy Radioelektroniki Ser. Obshchetekh.* **5** 124 (1978)
35. Berezhnov V V et al. *Akust. Zh.* **26** 328 (1980)
36. Berezhnov V V *Voprosy Radioelektroniki Ser. Obshchetekh.* **11** 121 (1982)
37. Kataev G I et al. *Zh. Eksp. Teor. Fiz.* **89** 1416 (1985) [*Sov. Phys. JETP* **62** 820 (1985)]
38. Dikshteĭn I E, Tarasenko V V, Kharitonov V D *Fiz. Tverd. Tela* (Leningrad) **21** 254 (1979) [*Sov. Phys. Solid State* **21** 152 (1979)]
39. Buchel'nikov V D, Shavrov V G *Fiz. Tverd. Tela* (Leningrad) **24** 909 (1982) [*Sov. Phys. Solid State* **24** 516 (1982)]
40. Buchel'nikov V D, Kuzavko Yu A, Shavrov V G *Fiz. Nizk. Temp.* **11** 1275 (1985) [*Sov. J. Low Temp. Phys.* **11** 705 (1985)]
41. Viktorov I A *Zvukovye Poverkhnostnye Volny v Tverdykh Telakh* (Surface Acoustic Waves in Solids) (Moscow: Nauka, 1981)
42. Deulesaint E, Royer D *Elastic Waves in Solids: Applications to Signal Processing* (Chichester: Wiley, 1980) [Translated into Russian (Moscow: Nauka, 1982)]
43. Balakirev M K, Gilinskiĭ I A *Volny v P'ezokristallakh* (Waves in Piezocrystals) (Novosibirsk: Nauka, 1982)
44. Biryukov S V et al. *Poverkhnostnye Akusticheskie Volny v Neodnorodnykh Sredakh* (Surface Acoustic Waves in Inhomogeneous Media) (Moscow: Nauka, 1991)
45. Gulyaev Yu V *Pis'ma Zh. Eksp. Teor. Fiz.* **9** 63 (1969) [*JETP Lett.* **9** 37 (1969)]
46. Bleustein J L *Appl. Phys. Lett.* **13** 412 (1968)
47. Eshbach J R, Damon R W *Phys. Rev.* **118** 1208 (1960)
48. Damon R W, Eshbach J R *J. Phys. Chem. Sol.* **19** 308 (1961)
49. Gann V V *Fiz. Tverd. Tela* (Leningrad) **8** 3167 (1966) [*Sov. Phys. Solid State* **8** 2537 (1967)]
50. Bulaevskiĭ L N *Fiz. Tverd. Tela* (Leningrad) **12** 799 (1970)
51. De Wames R E, Wolfram T *J. Appl. Phys.* **41** 987 (1970)
52. Khlebopros R G, Mikhailovskiĭ L V *Izv. Akad. Nauk SSSR Ser. Fiz.* **36** 1522 (1972) [*Bull. Acad. Sci. USSR Ser. Phys.*]
53. Filippov B N, Tityakov I G *Fiz. Met. Metalloved.* **35** 28 (1973)
54. Bespyatykh Yu I, Dikshteĭn I E, Tarasenko V V *Fiz. Tverd. Tela* (Leningrad) **22** 3335 (1980) [*Sov. Phys. Solid State* **22** 1953 (1980)]
55. Filippov B N *Fiz. Tverd. Tela* (Leningrad) **9** 1339 (1967)
56. Wallis R F et al. *Solid State Commun.* **5** 89 (1967)
57. Wolfram T, De Wames R E *Phys. Rev.* **185** 762 (1969)
58. Ivanov B A, Lapchenko V F, Sukstanskiĭ A L *Fiz. Tverd. Tela* (Leningrad) **27** 173 (1985)
59. Filippov B N, Onoprienko L G *Fiz. Met. Metalloved.* **30** 1121 (1970)
60. Parekh J P, Bertoni H L *Appl. Phys. Lett.* **20** 362 (1972)
61. Parekh J P, Bertoni H L *J. Appl. Phys.* **45** 434 (1974)
62. Parekh J P, Bertoni H L *J. Appl. Phys.* **45** 1860 (1974)
63. Scott R Q, Mills D L *Solid State Commun.* **18** 849 (1976)
64. Scott R Q, Mills D L *Phys. Rev. B* **15** 3545 (1977)
65. Camley R E, Scott R Q *Phys. Rev. B* **17** 4327 (1978)
66. Filippov B N, Preprint No. 80/1 (Sverdlovsk: Institute of Metal Physics, Ural Division, USSR Academy of Sciences, 1980)
67. Matthews H, Van de Vaart H *Appl. Phys. Lett.* **15** 373 (1969)
68. Parekh J P *Electron. Lett.* **6** 430 (1970)
69. Van de Vaart H *J. Appl. Phys.* **42** 5305 (1971)
70. Camley R E *J. Appl. Phys.* **50** 5272 (1979)
71. Parekh J P *Electron. Lett.* **6** 47 (1970)
72. Camley R E, Maradudin A A *Appl. Phys. Lett.* **38** 610 (1981)
73. Van de Vaart H, Matthews H *Appl. Phys. Lett.* **16** 153 (1970)
74. Filippov B N, Lukomskiĭ V P *Fiz. Met. Metalloved.* **34** 682 (1972)

75. Filippov B N, Boltachev V D, Lebedev Yu G *Fiz. Met. Metalloved.* **49** 1150 (1980)
76. Bugaev A S et al. *Fiz. Tverd. Tela* (Leningrad) **23** 2647 (1981) [*Sov. Phys. Solid State* **23** 1552 (1981)]
77. Bugaev A S et al. *Radiotekh. Elektron.* **27** 1979 (1982)
78. Kazakov G T, Tikhonov V V, Zil'berman P E *Fiz. Tverd. Tela* (Leningrad) **25** 2307 (1983) [*Sov. Phys. Solid State* **25** 1324 (1983)]
79. Andreev A S et al. *Pis'ma Zh. Tekh. Fiz.* **10** 90 (1984) [*Sov. Tech. Phys. Lett.* **10** 37 (1984)]
80. Andreev A S et al. *Radiotekh. Elektron.* **30** 1992 (1985)
81. Burlak G N, Kotsarenko N Ya, Rapoport Yu G *Ukr. Fiz. Zh.* (USSR) **30** 291 (1985)
82. Nechiporenko V N, Rapoport Yu G *Akust. Zh.* **31** 365 (1985) [*Sov. Phys. Acoust.* **31** 215 (1985)]
83. Gulyaev Yu V, Zil'berman P E *Izv. Vyssh. Uchebn. Zaved. Fiz.* **31** (11) 6 (1988) [*Sov. Phys. J.* **31** (11) 860 (1988)]
84. Parekh J P *Electron. Lett.* **5** 322 (1969)
85. Parekh J P *Electron. Lett.* **5** 540 (1969)
86. Kuzavko Yu A, Shavrov V G, in *Proc. 16th All-Union Conference on Physics of Magnetic Phenomena* Part 1 (Tula, 1983) Abstracts of Papers, p. 207
87. Gulyaev Yu V et al. *Zh. Eksp. Teor. Fiz.* **87** 674 (1984) [*Sov. Phys. JETP* **60** 386 (1984)]
88. Kuzavko Yu A, Oleinik I N, Shavrov V G *Fiz. Tverd. Tela* (Leningrad) **26** 3669 (1984) [*Sov. Phys. Solid State* **26** 2208 (1984)]
89. Gulyaev Yu V et al. *Acta Phys. Pol. A* **58** 289 (1980)
90. Gulyaev Yu V et al. *Fiz. Tverd. Tela* (Leningrad) **28** 1243 (1986) [*Sov. Phys. Solid State* **28** 701 (1986)]
91. Gulyaev Yu V, Kuzavko Yu A, Shavrov V G, in *Proc. of Int. Symp. Surface Waves in Solid and Layered Structures* Vol. 2 (Novosibirsk, 1986) p. 62
92. Kaganov M I, Kosevich Yu A *Poverkhnost* (8) 148 (1986)
93. Ioffe I V *Pis'ma Zh. Eksp. Teor. Fiz.* **36** 33 (1982) [*JETP Lett.* **36** 38 (1982)]
94. Vlasov K B *Zh. Eksp. Teor. Fiz.* **43** 2128 (1962) [*Sov. Phys. JETP* **16** 1505 (1963)]
95. Vlasov K B, Ishmukhametov B Kh *Zh. Eksp. Teor. Fiz.* **46** 201 (1964) [*Sov. Phys. JETP* **19** 142 (1964)]
96. Tiersten H F *J. Math. Phys.* **5** 1298 (1964)
97. Akhiezer A I, Bar'yakhtar V G, Peletminskiĭ S V *Spinovye Volny* (Spin Waves) (Moscow: Nauka, 1967) [Translated into English (New York: Interscience, 1968)]
98. Bar'yakhtar V G, Turov E A, in *Spin Waves and Magnetic Excitations* Ch. 7 (Eds A S Borovik-Romanov, S K Sinha) (Amsterdam: Elsevier, 1988)
99. Melcher R L *Phys. Rev. Lett.* **25** 1201 (1970)
100. Melcher R L, in *Enrico Fermi School* (Varenna, Course LII, 1972) (Ed. E Burstein) (New York: Academic Press,1972) p. 257
101. Eastman D E *Phys. Rev.* **148** 530 (1966)
102. Bar'yakhtar V G, Loktev V M, Ryabchenko S M *Zh. Eksp. Teor. Fiz.* **88** 1752 (1985) [*Sov. Phys. JETP* **61** 1040 (1985)]
103. Bar'yakhtar V G, Loktev V M *Fiz. Nizk. Temp.* **11** 1082 (1985) [*Sov. J. Low Temp. Phys.* **11** 597 (1985)]
104. Gerus S V, Tarasenko V V *Fiz. Tverd. Tela* (Leningrad) **17** 2247 (1975) [*Sov. Phys. Solid State* **17** 1487 (1976)]
105. Kukhtin Z I, Preobrazhenskiĭ V L, Ekonomov N A *Fiz. Tverd. Tela* (Leningrad) **26** 884 (1984) [*Sov. Phys. Solid State* **26** 536 (1984)]
106. Alekseev A N, Ermolov V A, Naumenko N F *Pis'ma Zh. Tekh. Fiz.* **10** 238 (1984) [*Sov. Tech. Phys. Lett.* **10** 99 (1984)]
107. Ermolov V A et al. *Fiz. Tverd. Tela* (Leningrad) **26** 2443 (1984) [*Sov. Phys. Solid State* **26** 1480 (1984)]
108. Pol'skiĭ A I et al. *Pis'ma Zh. Tekh. Fiz.* **11** 954 (1985) [*Sov. Phys. Tech. Phys. Lett.* **11** 395 (1985)]
109. Krasil'nikov V A, Mamatova T A, Prokoshev V G *Pis'ma Zh. Tekh. Fiz.* **10** 1196 (1984) [*Sov. Tech. Phys. Lett.* **10** 506 (1984)]
110. Gubkin M K, Mamatova T A, Prokoshev V G *Akust. Zh.* **31** 678 (1985) [*Sov. Phys. Acoust.* **31** 410 (1985)]
111. Ermolov V A, Alekseev A I, Pankratov V G *Pis'ma Zh. Tekh. Fiz.* **11** 277 (1985) [*Sov. Tech. Phys. Lett.* **11** 156 (1985)]
112. Buchel'nikov V D, Kuzavko Yu A, Shavrov V G *Akust. Zh.* **37** 892 (1991) [*Sov. Phys. Acoust.* **37** 464 (1991)]
113. Dikshteĭn I E *Fiz. Tverd. Tela* (Leningrad) **31** 175 (1989) [*Sov. Phys. Solid State* **31** 447 (1989)]
114. Dzyaloshinskiĭ I E *Zh. Eksp. Teor. Fiz.* **33** 807 (1957) [*Sov. Phys. JETP* **6** 621 (1958)]
115. Borovik-Romanov A S *Zh. Eksp. Teor. Fiz.* **36** 1954 (1959) [*Sov. Phys. JETP* **36** 1390 (1959)]
116. Mitsek A I, Shavrov V G *Fiz. Tverd. Tela* (Leningrad) **6** 210 (1964) [*Sov. Phys. Solid State* **6** 167 (1964)]
117. Kabychenkov A F, Shavrov V G *Fiz. Tverd. Tela* (Leningrad) **28** 433 (1986) [*Sov. Phys. Solid State* **28** 240 (1986)]
118. Moriya T *J. Phys. Chem. Solids* **11** 73 (1959)
119. Bar'yakhtar V G et al. *Zh. Eksp. Teor. Fiz.* **87** 1028 (1984) [*Sov. Phys. JETP* **60** 587 (1984)]
120. Gerus S V et al. *Fiz. Tverd. Tela* (Leningrad) **19** 218 (1977)
121. Borshchan V S, Manuilov M V, Serdobol'skaya O Yu *Fiz. Tverd. Tela* (Leningrad) **24** 932 (1982) [*Sov. Phys. Solid State* **24** 531 (1982)]
122. Borshchan V S, Manuilov M V, Serdobol'skaya O Yu *Fiz. Tverd. Tela* (Leningrad) **24** 935 (1982) [*Sov. Phys. Solid State* **24** 532 (1982)]
123. Borshchan V S et al. *Fiz. Tverd. Tela* (Leningrad) **24** 2574 (1982) [*Sov. Phys. Solid State* **24** 1460 (1982)]
124. Borshchan V S, Serdobol'skaya O Yu *Izv. Akad. Nauk SSSR Ser. Fiz.* **49** 279 (1985) [*Bull. Acad. Sci. USSR Ser. Phys.* **49** 61 (1985)]
125. Bar'yakhtar V G, Obozhin I I, Khudik B I, Preprint No. 86-80-P (Kiev: ITF, 1986)
126. Lifshitz I M *Zh. Eksp. Teor. Fiz.* **22** 475 (1952)
127. Buchel'nikov V D, Shavrov V G *Fiz. Tverd. Tela* (Leningrad) **25** 90 (1983) [*Sov. Phys. Solid State* **25** 49 (1983)]
128. Vlasko-Vlasov V K, Khapikov A F *Zh. Eksp. Teor. Fiz.* **93** 1508 (1987) [*Sov. Phys. JETP* **66** 861 (1987)]
129. Kabychenkov A F, Shavrov V G *Acta Phys. Pol. A* **73** 531 (1988)
130. Kabychenkov A F, Shavrov V G *Zh. Eksp. Teor. Fiz.* **95** 580 (1989) [*Sov. Phys. JETP* **68** 326 (1989)]
131. Kabychenkov A F, Shavrov V G, Shevchenko A L *Fiz. Tverd. Tela* (Leningrad) **32** 2010 (1990) [*Sov. Phys. Solid State* **32** 1170 (1990)]
132. Gerasimchuk V S, Sukstanskiĭ A L *Zh. Eksp. Teor. Fiz.* **103** 151 (1993) [*JETP* **76** 82 (1993)]
133. Cherechukin A A et al., in *Proc. of the Int. Symp. on Nonlinear Electromagnetic Systems* (Cardiff, Wales, UK, 1995) p. 438
134. Bespyatykh Yu I, Dikshteĭn I E, Tarasenko V V *Fiz. Tverd. Tela* (Leningrad) **23** 3013 (1981) [*Sov. Phys. Solid State* **23** 1757 (1981)]
135. Dikshteĭn I E *Fiz. Tverd. Tela* (Leningrad) **32** 1286 (1990) [*Sov. Phys. Solid State* **32** 754 (1990)]